SURFACE ROUGHNESS OF LITHIUM DISILICATE GLASS CERAMICS BEFORE AND AFTER CRYSTALLIZATION WITH DIFFERENT MILLING TECHNIQUES:

WET VS SUBMERGED MILLING

SHARON WONG KAH KHEI

FACULTY OF DENTISTRY
UNIVERSITI MALAYA
KUALA LUMPUR

2024

SURFACE ROUGHNESS OF LITHIUM DISILICATE GLASS CERAMICS BEFORE AND AFTER CRYSTALLIZATION WITH DIFFERENT MILLING TECHNIQUES:

WET VS SUBMERGED MILLING

SHARON WONG KAH KHEI

RESEARCH REPORT SUBMITTED TO THE FACULTY OF DENTISTRY, UNIVERSITI MALAYA, IN PARTIAL FULFILMENT OF THE REQUIREMENTS FOR THE DEGREE OF MASTER OF ORAL SCIENCE

FACULTY OF DENTISTRY
UNIVERSITI MALAYA
KUALA LUMPUR

2024

UNIVERSITY MALAYA

ORIGINAL LITERARY WORK DECLARATION

Name of Candidate: Sharon Wong Kah Khei

Registration/Matric No: S2031389

Name of Degree: Master of Oral Science (Restorative)

Title of Project Paper/Research Report/Dissertation/Thesis ("this Work"):

Surface Roughness of Lithium Disilicate Glass Ceramics Before and After Crystallization with Different Milling Techniques: Wet Vs Submerged Milling

Field of Study: Dental material

I do solemnly and sincerely declare that:

(1) I am the sole author/writer of this Work;
(2) This Work is original;
(3) Any use of any work in which copyright exists was done by way of fair dealing and for permitted purposes and any excerpt or extract from, or reference to or reproduction of any copyright work has been disclosed expressly and sufficiently and the title of the Work and its authorship have been acknowledged in this Work;
(4) I do not have any actual knowledge nor do I ought reasonably to know that the making of this work constitutes an infringement of any copyright work;
(5) I hereby assign all and every rights in the copyright to this Work to the University of Malaya ("UM"), who henceforth shall be owner of the copyright in this Work and that any reproduction or use in any form or by any means whatsoever is prohibited without the written consent of UM having been first had and obtained;
(6) I am fully aware that if in the course of making this Work, I have infringed any copyright whether intentionally or otherwise, I may be subject to legal action or any other action as may be determined by UM.

Candidate's Signature Date: 25/9/2024

Subscribed and solemnly declared before,

Witness's Signature Date: 25/9/2024

Name:

Designation:

SURFACE ROUGHNESS OF LITHIUM DISILICATE GLASS CERAMICS BEFORE AND AFTER CRYSTALLIZATION WITH DIFFERENT MILLING TECHNIQUES: WET VS SUBMERGED MILLING

ABSTRACT

This study investigates the impact of wet milling and submerged milling on the surface roughness of milled lithium disilicate glass ceramic with sequential milling and before and after crystallization process. Submerged milling is gaining traction for its potential to dissipate heat, reduce friction, remove debris more efficiently, increase milling tool longevity, and ensure accurate and efficient milling of final products. A total of 24 Hass Amber® Mill lithium disilicate blocks were divided into 2 groups according to different milling methods: wet milling group (n = 12) and submerged milling group (n = 12). The milling process was performed using a 5-axis CRAFT 5X milling machine. The milled surfaces of the lithium disilicate glass ceramic were evaluated for surface roughness (Ra) using a 3D optical non-contact surface profilometer and observed through Scanning Electron Microscopy (SEM), both before and after the crystallization process. The diamond-coated milling burs (GC 25, GC 20, GC 10) were initially observed under SEM and at 1st, 6th, and 12th milling. Overall comparisons between the surface roughness of lithium disilicate discs of the two groups were done using Paired T-test. Comparisons between the surface roughness of the disc before and after crystallization were done using Paired T-test. The comparison of surface roughness intragroup was done using one-way ANOVA. Significance was set at p value < 0.05. Results indicated that the mean surface roughness of lithium disilicate discs milled with submerged milling technique was significantly lower than that of wet milled discs, both before ($p < 0.001$, $t = 7.093$) and after crystallization ($p < 0.001$, $t = 6.020$). Within each milling group, Ra reduced after crystallization, with significant differences pre- and post-crystallization (wet: $p < 0.001$,

t = 3.344; submerged: $p < 0.001$, t = 4.683). One-way ANOVA results showed that there was no significant difference in surface roughness between discs in the same group ($p > 0.05$ for all groups), suggesting that the 12-cycle milling sequence did not significantly affect the surface roughness. SEM analysis showed loss of abrasive particles on milling bur in both wet and submerged milling groups. This study concludes that submerged milling is more effective in reducing surface roughness compared to wet milling and that crystallization plays a crucial role in further reducing the surface roughness of lithium disilicate glass ceramics. Also, using sequential milling tool usage up to the 12th mill did not affect the surface roughness of milled lithium disilicate.

Keywords: lithium disilicate, Computer-Aided Design/ Computer Aided Manufacturing (CAD/CAM), wet milling, submerged milling, surface roughness

KEKASARAN PERMUKAAN SERAMIK KACA LITIUM DISILIKAT SEBELUM DAN SELEPAS PENGHABLURAN DENGAN TEKNIK PENGISARAN YANG BERBEZA: PENGISARAN BASAH VS TERENDAM

ABSTRAK

Kajian ini menyiasat kesan pengilangan basah dan pengilangan tenggelam ke atas kekasaran permukaan seramik kaca litium disilikat giling dengan pengilangan berjujukan dan sebelum dan selepas proses penghabluran. Pengilangan terendam semakin mendapat daya tarikan kerana potensinya untuk menghilangkan haba, mengurangkan geseran, membuang serpihan dengan lebih cekap, meningkatkan umur panjang alat pengilangan, dan memastikan pengilangan produk akhir yang tepat dan cekap. Sebanyak 24 blok litium disilikat Hass Amber® Mill dibahagikan kepada 2 kumpulan mengikut kaedah pengilangan yang berbeza: kumpulan pengilangan basah (n = 12) dan kumpulan pengilangan terendam (n = 12). Proses pengilangan dilakukan menggunakan mesin pengisar 5-axis CRAFT 5X. Permukaan giling seramik kaca litium disilikat dinilai untuk kekasaran permukaan (Ra) menggunakan profilometer permukaan bukan sentuhan optik 3D dan diperhatikan melalui Scanning Electron Microscopy (SEM), sebelum dan selepas proses penghabluran. Burs pengilangan bersalut berlian (GC 25, GC 20, GC 10) pada mulanya diperhatikan di bawah SEM dan pada pengilangan ke-1, ke-6, dan ke-12. Perbandingan keseluruhan antara kekasaran permukaan cakera litium disilikat kedua-dua kumpulan dilakukan menggunakan ujian T Berpasangan. Perbandingan antara kekasaran permukaan cakera sebelum dan selepas penghabluran dilakukan menggunakan ujian T Berpasangan. Perbandingan intrakumpulan kekasaran permukaan dilakukan menggunakan ANOVA sehala. Kepentingan ditetapkan pada nilai $p < 0.05$. Keputusan menunjukkan bahawa purata kekasaran permukaan cakera litium disilikat yang digiling dengan teknik pengilangan tenggelam adalah jauh lebih rendah daripada cakera giling basah, kedua-duanya sebelum ($p < 0.001$, $t = 7.093$) dan selepas penghabluran ($p < 0.001$,

t = 6.020). Dalam setiap kumpulan pengilangan, Ra berkurangan selepas penghabluran, dengan perbezaan ketara sebelum dan selepas penghabluran (basah: $p < 0.001$, $t = 3.344$; tenggelam: $p < 0.001$, $t = 4.683$). Keputusan ANOVA sehala menunjukkan bahawa tidak terdapat perbezaan yang signifikan dalam kekasaran permukaan antara cakera dalam kumpulan yang sama ($p > 0.05$ untuk semua kumpulan), menunjukkan bahawa jujukan pengilangan 12 kitaran tidak memberi kesan ketara ke atas kekasaran permukaan. Analisis SEM menunjukkan kehilangan zarah kasar pada bur penggilingan dalam kedua-dua kumpulan pengilangan basah dan tenggelam. Kajian ini menyimpulkan bahawa pengilangan terendam adalah lebih berkesan dalam mengurangkan kekasaran permukaan berbanding dengan pengilangan basah dan penghabluran memainkan peranan penting dalam mengurangkan lagi kekasaran permukaan seramik kaca litium disilikat. Selain itu, penggunaan alat pengilangan berjujukan sehingga kilang ke-12 tidak menjejaskan kekasaran permukaan litium disilikat yang dikisar.

Kata kunci: disilikat litium, Rekabentuk berbantu komputer/ pembuatan berbantu komputer (CAD/CAM), pengisaran basah, pengisaran tenggelam, kekasaran permukaan

ACKNOWLEDGEMENTS

I would like to extend my heartfelt appreciation to the individuals and institutions that have played a crucial part in the successful completion of my thesis. I would like to express my utmost gratitude to my supervisors, Dr. Yeoh Oon Take, Prof. Dr. Chai Wen Lin, and Dr. Sofya binti Zulkiffli, for their unwavering support and excellent mentorship. Their combined knowledge and expertise have been invaluable in shaping the direction, progress, and improvement of this research.

Special acknowledgements are extended to Dr. Muralithran A/L Govindan Kutty for his expert insights in the field of material science and Dr. Alias Abd Aziz for his guidance on the statistical part of this study.

I would like to thank the staff members and technicians of the Biomaterial Research Laboratory (BRL) (UM), Postgraduate Dental Technology Laboratory (UM), MIMOS Berhad, and DOF SEA Sdn Bhd for their unwavering help and support. Their assistance has been crucial in navigating the challenges and complexities of my research. I'm also deeply appreciative of my colleagues and friends for their continuous encouragement and advice.

In addition to academic and institutional support, I would like to thank my parents and my partner for their endless support and understanding throughout this academic journey.

Lastly, I want to acknowledge my two feline companions, Daisy and Dee, for their role in relieving stress and enhancing my overall mental well-being. Their presence has provided solace during intense periods of research and writing.

TABLE OF CONTENTS

LIST OF FIGURES

LIST OF TABLES

LIST OF SYMBOLS AND ABBREVIATIONS

%	:	Percent
CAD/CAM	:	Computer aided design/Computer aided manufacturing
HT	:	High translucency
Ra	:	Average roughness
Sa	:	Areal average roughness
SEM	:	Scanning electron microscope

LIST OF APPENDICES

CHAPTER 1: INTRODUCTION

1.1 Research Background

Computer-Aided Design (CAD) and Computer-Aided Manufacturing (CAM) have transformed the field of dentistry in the past five decades (Duret et al., 1988) particularly in the fabrication of dental prostheses. This approach offers several advantages, including high precision, efficiency, and accuracy, leading to a reduction in overall processing time (Miyazaki et al., 2009).

Glass ceramic material, particularly lithium disilicate ($Li_2 Si_2 O_5$), has been widely used in CAD/CAM for creating indirect restorations in dentistry due to their superior aesthetics and higher mechanical properties compared to other glass ceramics (Sailer et al., 2015). Lithium disilicate prostheses are manufactured by milling of intermediate lithium metasilicate ($Li_2 Si O_3$), followed by sintering to transform into lithium disilicate crystals (Alao et al., 2017; Ortiz et al., 2019). This is because lithium metasilicate has lower strength than lithium disilicate, making it easier to mill with diamond tools and reducing wear of machining devices at the same time (Alao et al., 2017; Denry & Holloway, 2010). However, the fabrication of all-ceramic restoration using CAD/CAM mainly involves controlled reduction of premanufactured CAD/CAM blocks using milling bur, which results in strength-limiting surface and subsurface damage in the milled prosthesis (Pilecco et al., 2021). Therefore, milling conditions and milling tools are crucial to reduce surface flaws and maintain the restoration's quality and durability.

Cooling and lubrication are essential when milling hard materials, aiding in heat dissipation, friction reduction, reduced milling tool wear, and the removal of cutting debris from the cutting zone. In dentistry, CAD/CAM technology may utilise different

types of cooling and lubricating processes, depending on the type of restoration. These methods include compressed air (dry milling), water spray or mist (wet milling), and flood coolant (submerged milling). Wet milling involves the controlled use of a liquid coolant in the form of a water spray during milling, while submerged milling involves the immersion of the entire material in a tank with constantly flowing lubricating liquid during the milling process.

According to the manufacturer's claim, submerged milling is capable of dissipating heat, reducing friction, and removing debris more efficiently when compared to wet milling. This is supposed to increase tool longevity and ensure accurate and efficient milling of glass ceramic for a more durable final product (CAD-Ray, 2023). Submerged milling can be advantageous to manufacture glass ceramic restorations with improved properties. However, since submerged milling is a relatively novel milling technique in the dental industry, there is currently insufficient literature to define its superiority over wet milling in the production of glass ceramic-based prostheses, particularly those made from lithium disilicate.

To address this research gap, this study aimed to investigate the impact of two different milling techniques, namely wet milling and submerged milling, on the surface roughness of milled lithium disilicate and to compare before and after the crystallization process. Additionally, this study also investigates the surface roughness of lithium disilicate and observes the morphology of milling tools following sequential usage for both milling strategies. These can provide valuable insights into the comparative effectiveness of these milling methods and contribute to a more comprehensive understanding of their influence on the surface quality of lithium disilicate glass ceramics.

1.2 Aim

The aim of this study is to evaluate the effect of two different milling techniques: wet milling and submerged milling, on the surface roughness (Ra) of milled lithium disilicate before and after crystallization.

1.3 Objectives

i. To compare the surface roughness of lithium disilicate milled using wet milling and submerged milling techniques.

ii. To assess the effect of crystallization on the surface roughness of milled lithium disilicate for both wet and submerged milling techniques.

iii. To determine the impact of sequential milling tool usage on the surface roughness of lithium disilicate for both wet and submerged milling techniques.

1.4 Null hypotheses

i. There will be no significant difference in the surface roughness of milled lithium disilicate between wet and submerged milling techniques.

ii. Crystallization will not have a significant effect on the surface roughness of lithium disilicate in wet and submerged milling techniques.

iii. Sequential milling tool usage using wet and submerged milling techniques has no impact on the surface roughness of lithium disilicate

1.5 Significance of the study

There is a lack of scientific evidence regarding the superiority of submerged milling over conventional wet milling for lithium disilicate-based prosthesis manufacturing. Hence, the scientific evidence presented in this study will serve as a valuable resource for clinicians and laboratories, aiding them in selecting the most effective milling technique for restoration with reduced surface roughness. The findings are expected to contribute to the scientific community through research publications, as well as provide recommendations for specific applications in dental laboratories and chairside milling.

CHAPTER 2: LITERATURE REVIEW

2.1 Glass Ceramics

Synthetic glass ceramic was invented in 1953 by Stanley Donald Stookey at Corning Glass Works (Fu et al., 2016). This groundbreaking discovery was the result of a series of events, starting with annealing a piece of lithium disilicate glass with precipitated silver particles (meant to form permanent photographic images) in an overheating furnace due to a malfunctioning temperature controller. It was observed that the fired sample did not shatter upon dropping onto a concrete floor (Zanotto, 2010). This marked the first incidental glass ceramic creation in history.

Subsequently, glass ceramics were applied in fabricating products such as cookware, advanced electronic devices, optical components, chemical systems, mechanical apparatus, aerospace components, and implant surgery. Their application in prosthetic dentistry was particularly significant. (James, 1995; Zanotto, 2010).

Glass ceramic is defined as a solid material, crystalline and partly glassy, formed by controlled crystallization of glass (Ferro et al., 2017). According to the classification system for all ceramic and ceramic-like dental restoration materials by Gracis et al. in 2015, glass-matrix ceramics can be divided into feldspathic, synthetic (leucite-based, lithium disilicate and derivatives, fluorapatite-based), and glass-infiltrated (alumina, alumina and magnesium, alumina and zirconia) (Gracis et al., 2015).

2.2 Lithium disilicate

2.2.1 History of lithium disilicate

The introduction of lithium disilicate glass ceramic material to the dental community marked a significant advancement in restorative dentistry. Initially, the fabrication process involved the use of the lost wax technique, followed by heat pressing to form the final restoration. The CAD version was introduced in 2006. The widespread acceptance and growing popularity over the past few decades can be attributed to its remarkable biocompatibility, high flexural strength, superior aesthetics and translucency qualities, and adhesive bonding ability to enamel and dentin (Lindner et al., 2023).

Lithium disilicate glass ceramics demonstrated exceptional versatility in various dental applications, including single restorations for both anterior and posterior teeth and 3-unit fixed dental prostheses to replace teeth up to the second premolar. The introduction of contemporary adhesive procedures has made it possible to move away from retentive preparation designs, thereby enabling the preservation of the residual tooth structure (Ahlers et al., 2009; Fuzzi & Rappelli, 1998). With a minimal ceramic thickness of 1 mm in load-bearing areas, preparation designs can be optimized for maximal tooth preservation. This allows for minimally invasive treatment procedures to be adopted in modern restorative dentistry (Nawafleh et al., 2017; Sasse et al., 2015; Seydler et al., 2014).

Lithium disilicate (SiO_2-Li_2O) glass ceramics were introduced in 1998 with the release of IPS Empress 2 (Ivoclar Vivadent, Lichtenstein). It was comprised of approximately 65% crystalline lithium disilicate filler, 34% glass, and 1% pore (Guazzato et al., 2004). This heat-pressed glass ceramic can be utilized as a core material that is layered with fluorapatite-based ceramics. An improved version was introduced in 2005 with superior

optical and mechanical properties in comparison to the IPS Empress 2. With the introduction of this IPS e.max Press, IPS Empress 2 was discontinued in 2009. The crystals in the IPS e.max Press are smaller and more uniformly distributed. This versatile material is able to produce anatomically shaped, monolithic restorations without the need for veneering ceramic.

The subsequent patent expiration of IPS e.max Press and IPS e.max CAD has resulted in the emergence of generic variants in the market. Some examples of pressable lithium disilicate-based ceramics are Amber Press (HassBio, Gangwon-do, Korea), Amber Press Master (HassBio, Gangwon-do, Korea), GC Initial LiSi Press (GC, Tokyo, Japan), Vintage LD Press (Shofu, Kyoto, Japan), and VITA Ambria (VITA Zahnfabrik, Bad Säckingen, Germany) (Phark & Duarte, 2022).

2.2.2 Production of lithium disilicate restoration with CAD/CAM

CAD/CAM workflow is a revolutionary innovation that improves the design and production of various types of dental restorations, such as crowns, veneers, inlays, onlays, fixed bridges, implants, dentures, and orthodontic appliances (Mörmann & Brandestini, 1987). This technology, which was first introduced in the 1980s, greatly improved the use of digital workflow in the dental prostheses fabrication (Mörmann, 2006). The CAD/CAM workflow consists of three key steps. The first step is digitalization of impression, which converts geometric information into a digital format that can be processed by the computer. The second step involves virtual design, which generates the geometric shape for dental prosthesis. The third step is a prosthesis production that utilizes additive or subtractive strategies to create the final prostheses (Mörmann, 2006).

As the use of digital dentistry workflows became more popular, IPS e.max CAD was introduced in 2006 to fit into the digital workflow (Zarone et al., 2016). IPS e.max CAD (Ivoclar Vivadent, 2005) is manufactured in partially precrystallized blocks or "blue state" and is composed of 40% lithium metasilicate (Li_2SiO_3) crystals and lithium disilicate ($Li_2Si_2O_5$) crystal nuclei. Initially, the blocks show moderate hardness and strength (130 ± 30 MPa) which facilitates milling and to reduce wear of machining devices. Upon completion of milling, the restorations undergo further crystallization to achieve shade and strength (360 ± 60 MPa).

Machinable lithium disilicate-based ceramics used with CAD/CAM include Amber Mill (HassBio, Kangneung, Korea), Rosetta SM (HassBio, Kangneung, Korea), n!ce (Straumann, Freiburg, Germany), CEREC Tessera (Dentsply Sirona, York, PA, USA) and GC Initial LiSi Block (GC, Tokyo, Japan) (Phark & Duarte, 2022). The continuous advancement of these materials showcases the dedication to improve dental materials and patient outcomes in restorative dentistry.

2.2.3 Surface roughness of lithium disilicate

Surface roughness influences surface texture and it has an important role in determining how an object will interact with its environment (Al-Marzok & Al-Azzawi, 2009). Achieving a smooth surface on a direct or indirect restoration has multiple benefits, in particular to improve aesthetics and to prevent superficial staining and plaque accumulation. This, in turn, helps to prevent recurrent caries and periodontal disease (Yap et al., 1997).

Brittle dental materials tend to develop cracks and scratches (Bollen et al., 1996; Pacha-Olivenza et al., 2019). A few studies have shown that fractures of ceramic restoration

often originated from surface defects that were introduced during CAD/CAM milling (Fraga et al., 2017; Madruga et al., 2019; Pereira et al., 2016; Thompson & Rekow, 2004). The presence of these defects is attributed to the manufacturing process, and their propagation are influenced by the ceramic microstructures.

2.2.4 Crystallization of lithium disilicate

Lithium disilicate glass ceramics contain silicon dioxide matrix (silica or quartz) with embedded crystals (Gracis et al., 2015). Glass matrix alone does not offer adequate resistance against crack development and subsequent crack propagation that leads to inferior mechanical characteristics. However, dispersing lithium disilicate crystals into the glass matrix can reduce crack growth. Dispersion toughening strengthens glass matrix ceramic by improving its flexural strength and fracture toughness through the introduction of natural or synthetic crystals into the glass matrix (Kelly & Benetti, 2011). For leucite or lithium disilicate glass ceramics, crystals were grown internally through crystallization within the glassy matrix (Gracis et al., 2015).

Lithium disilicate is based on quartz-lithium dioxide binary phases. Phosphorous pentoxide (P_2O_5) is used as nucleation agent. Other raw powders like aluminum oxide (Al_2O_3), potassium oxide (K_2O), aluminum metaphosphate ($Al[PO_3]_3$), zirconium dioxide (ZrO_2), zinc oxide (ZnO), calcium oxide (CaO), vanadium pentoxide (V_2O_5), and cerium dioxide (CeO_2) are added to the base glass mix to improve chemical durability, mechanical strength, and optical properties (Phark & Duarte, 2022). All these components require a careful, heterogenous crystallisation procedure that begins with nucleation and crystal growth. These temperature-dependent and complex processes occur in different stages, depending on mode of fabrication. Heat-pressed LDCs are processed in two stages, while CAD/CAM milling blocks undergo three-stage process.

Both procedures begin with the manufacturer compacting or pressure casting glass base powders into moulds to form glass blocks or ingots. After cooling to 450-550°C, the glass melt is kept in a furnace for up to 1 hour to relax and induce nucleation of lithium silicate phases in the form of nano-lithium orthophosphate nuclei (Phark & Duarte, 2022).

For the three-stage crystallisation of machinable blocks (IPS e.max CAD), the second phase involves heating the glass block at 690-710°C for 10-30 min. This will cause epitaxial growth of lithium metasilicate (Li_2SiO_3) from the nuclei. After cooling, the block will contain about 40% of the intermediate metasilicate phase, evenly distributed as small platelet-like crystals. At this stage, the material is still weak (130 MPa flexural strength) but can be milled. In the third phase, the milling restoration is heated in a dental lab or clinician office at a temperature range of 820 °C to 850 °C for a duration of 20-30 minutes. The specific heating time and temperature rely on the chemical composition of the lithium disilicate based glass ceramics and are optimized by each manufacturer to achieve the desired properties (Alves et al., 2019). This solid-state interaction between lithium metasilicate crystals and surrounding silica creates 1.5 μm long, rod-like lithium disilicate crystals. These crystals further increase in size after heat treatment as observed in some studies (Fabian Fonzar et al., 2017; Hallmann et al., 2019). When fully crystallised, the lithium disilicate phase ($Li_2Si_2O_5$) occupies up to 70% of the volume (Höland et al., 2000). A little amount of lithium orthophosphate (Li_3PO_4) crystals and the glassy matrix remain (Duarte Jr et al., 2010). The restoration shrinks about 0.2% during the final sintering phase, but this is compensated by CAD programme automatically (Phark & Duarte, 2022). The crystallization of lithium disilicate is a critical stage after miling process, as it has a significant impact on the final properties (Miranda et al., 2020; Riquieri et al., 2018).

Belli et al. demonstrated that in two-step lithium silicate materials, the machining cracks that occur in the precrystallization state can reduce size of cracks during crystallization firing (Belli et al., 2019). This process also reduces brittleness caused by superficial microcracks and relieves stresses generated during machining (Belli et al., 2019; Hung et al., 2008), improves the flexural strength and fracture toughness (Lien et al., 2015), and aids in adjusting the optical/aesthetic properties of the material.

2.3 Milling techniques

2.3.1 Submerged milling

Cooling and lubrication are essential when milling hard materials, aiding in heat dissipation, friction reduction, the removal of cutting debris from the cutting zone and offer corrosion protection with the addition of corrosion inhibitors (Zheng Yang et al., 2023). Submerged coolant system provides a continuous flow of the coolant through the cutting zone. In this process, the work piece is positioned within a container and subsequently immersed in coolant. This ensures a layer of coolant will always be present above the work piece. Since the coolant is confined within a container, no coolant will be wasted due to splashing nor is there a need for cleaning in the flood coolant system. Additionally, this technique also leads to a better surface finish as the coolant is always present at the interface between the tool and the work piece (Naik et al., 2015).

2.3.2 Milling tool

In the manufacturing industry, the condition of the cutting tool plays a crucial part in attaining the desired level of quality in product. The primary challenge encountered by the cutting tool is its exposure to high operating temperatures resulting from the friction between the cutting tool and the component (Naik et al., 2015). At higher temperatures, the cutting tool experiences a decrease in its qualities, including hardness and strength.

This leads to a decrease in the dimensional accuracy of the component and a shorter lifespan of the tool (Dhar, 2005; Dhar et al., 2007).

The milling of CAD/CAM restorations involves the use of diamond burs, which inherently introduce surface alterations, including increased surface roughness and critical defects on the ceramic surface (Owen Addison et al., 2012; Quinn et al., 2005). A study conducted by Tomita et al. (2005) demonstrated that repeated use of milling diamond bur after 11^{th} to 21^{st} times of machining leads to the loss of diamond abrasive particles (Tomita et al., 2005). Previous in vitro studies have highlighted that these defects on the cementation surface act as stress concentrators, potentially leading to increase in crack dimension (Corazza et al., 2015; Turon-Vinas & Anglada, 2018). This can modifies the ceramic surface pattern and can impact the fatigue behaviour of the ceramic (Owen Addison et al., 2012; Corazza et al., 2015).

2.3.3 Effect of Sequential milling on surface roughness of glass ceramics

Study conducted by Yara (2005) found that the average surface roughness of ceramic crowns significantly increased with an increase in the number of machining times of milling diamond burs. The aforementioned study also concluded that there was a significant positive correlation between average surface roughness and number of diamond particle on the bur. The loss of active particles in diamond burs used in dentistry occurs as a result of repetitive cavity preparation or grinding (Yara et al., 2005). Similarly, another study conducted by Simba et al. (2022) examined the microstructure of cutting tools and found that the presence of diamond particles on the surface decreased with increasing accumulated usage time. As a result, the surface roughness of lithium disilicate and lithium metasilicate blocks increased when worn tools were used (Simba et al., 2022).

In contrast, a study by Madruga et al. (2019) observed that the sequential usage of diamond burs up to 18 cycles of CAD/CAM milling did not have a statistically significant influence on the roughness, topography, or fatigue strength of the ceramic discs (Madruga et al., 2019). Payaminia et al. (2021) likewise come to the conclusion that repeated use of a bur up to 10 milling cycles did not impact the surface roughness of leucite-reinforced glass ceramics (Payaminia et al., 2021b). Additionally, a study conducted by Addison et al. (2012) found no significant association between 14 cycles machining order of feldspathic ceramic (as an indirect measure of bur deterioration) and the surface roughness (Ra) value (O. Addison et al., 2012).

CHAPTER 3: MATERIALS AND METHODS

3.1 Sample size calculation

Sample size calculation was done using G*Power 3.1.9 with effect size d of 0.5, $\alpha = 0.05$ and power of study $(1 - \beta) = 80\%$ which was obtained from a previous study (Brodine et al., 2021). The sample size determined for surface roughness assessment is 64 (N = 64) per group. The sample size determination was also referenced from previous studies, which range from 10 to 14 specimens per group (Owen Addison et al., 2012; Brodine et al., 2021; Payaminia et al., 2021a). For our pilot study, the total number of specimens was 12 per group, with 5 readings per specimens (N = 60, n = 12).

3.2 Research Methodology Workflow

A brief outline of the methodology is illustrated as in Figure 3.1.

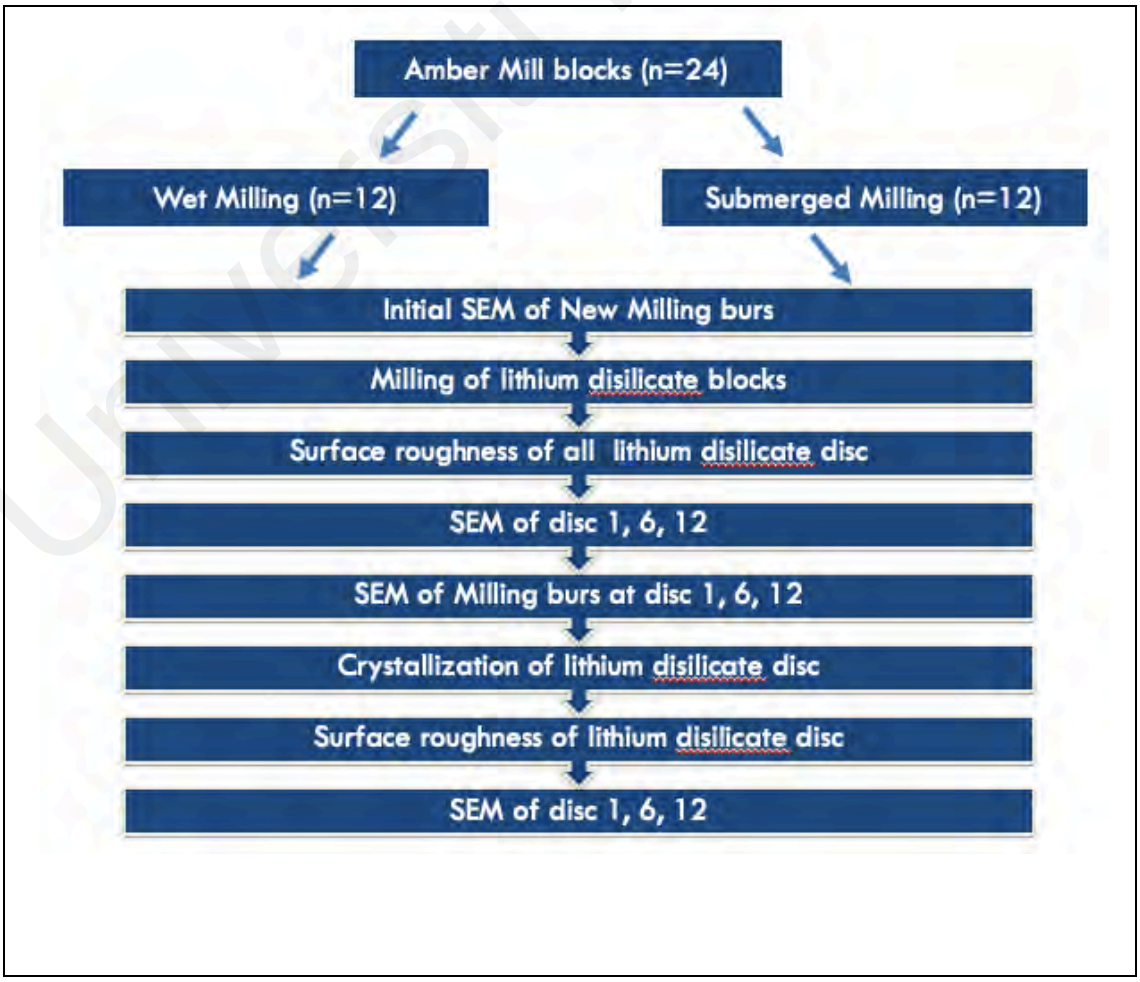

Figure 3.1: Research methodology workflow

3.3 Selection of materials

3.3.1 Lithium disilicate blocks

In this study, 24 blocks of Amber ® Mill lithium disilicate (HassBio, Kangneung, Korea) in shade A1 with composition of SiO_2 and Li_2O were used (Figure 3.2). Each block had a dimension of 18 mm x 14.5 mm x 12.3 mm. They were divided into 2 groups, where each group contained 12 blocks (n = 12) of lithium disilicate based ceramics.

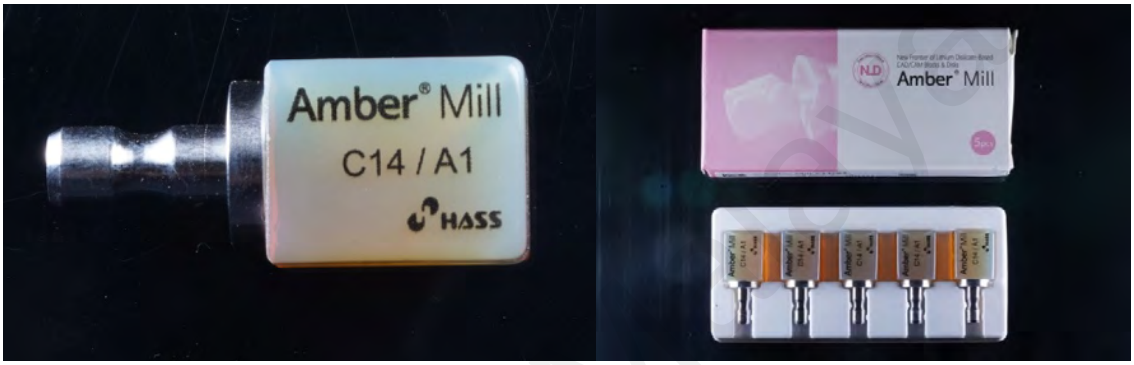

Figure 3.2: Amber® Mill lithium disilicate-based CAD/CAM blocks

3.3.2 Milling tools

One dedicated set for glass ceramic milling came with 3 milling tools (DOF Inc, Korea), namely GC 25 (Diamond-coated tool, diameter 25 mm) for cutting, GC 20 (Diamond-coated tool, diameter 20 mm) for machining, and GC 10 (Diamond-coated tool, diameter 10 mm) for finishing (Figure 3.3).

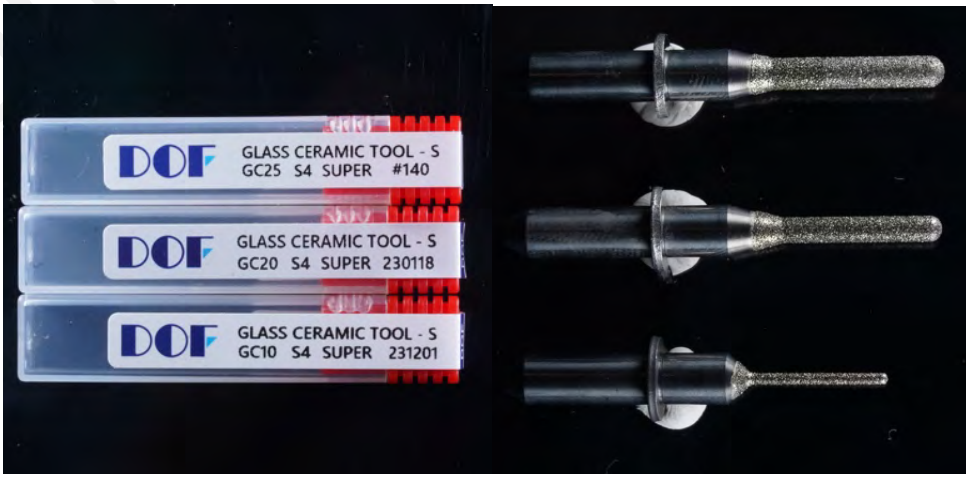

Figure 3.3: Glass ceramic tools GC 25, GC 20, GC 10

3.3.3 Milling machine

In this experiment, the milling machine being utilized was CRAFT 5X (DOF Inc, Korea), which is a 5-axis milling machine that was commercialized in the year 2022 (Figure 3.4A). The milling machine comes with a detachable submerged tank (launched early 2023) (Figure 3.4B) and is capable of doing dry, wet and submerged milling.

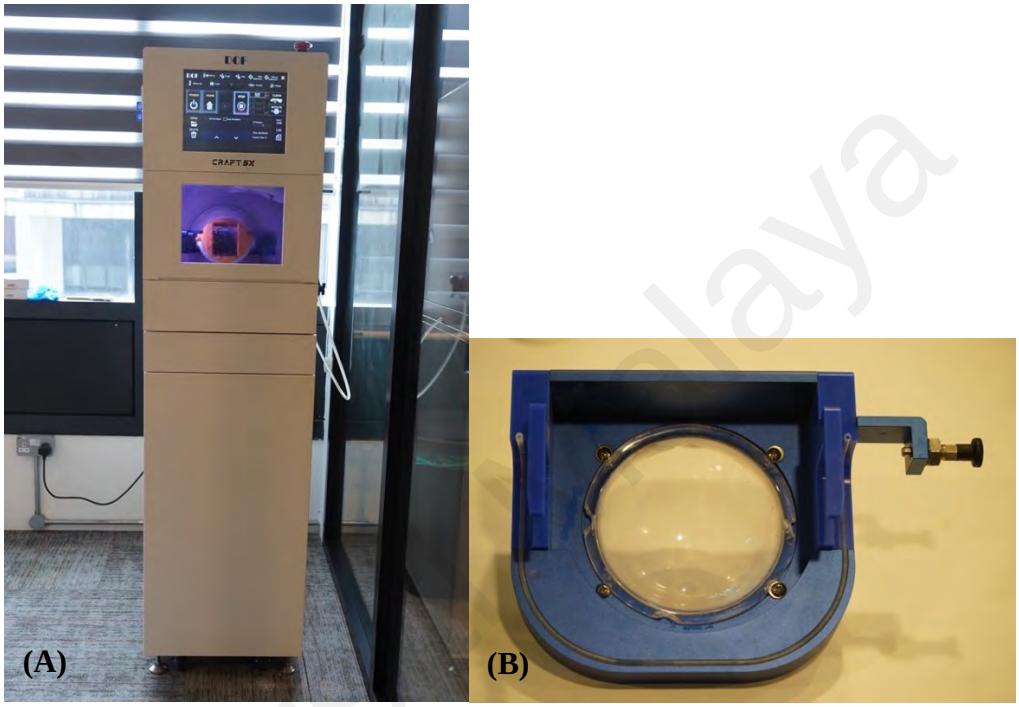

Figure 3.4: (A) CRAFT 5X milling machine; (B) Detachable submerged milling tank

3.4 Specimen preparation

A flat disc shaped specimen was designed by Blender software (version 4.0.2). Blender for dental is a CAD software used to virtually design teeth on scanned models and generate STL files (Figure 3.5A). The completed 3D design files were processed using the Computer Numeric Control (CNC) milling software, specifically the Millbox (version 2024) for CRAFT 5X program by DOF.Inc (Figure 3.5B).

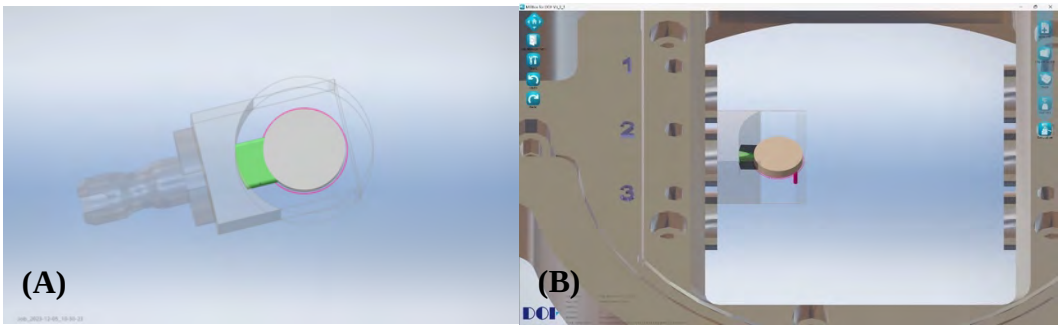

Figure 3.5: (A) Blender software to design disc-shaped specimen; (B) Millbox software to position the disc for milling

24 lithium disilicate blocks were divided into 2 groups and were milled accordingly:

Group A: 12 Hass Amber ® Mill lithium disilicate milled with default water coolant (wet milling- Figure 3.6A)

Group B: 12 Hass Amber ® lithium disilicate milled with detachable tank (submerged milling- Figure 3.6B)

Each group was milled with new sets of milling tools and the milling was done with the milling machine. The machining strategy was set to "Standard" (comprising Roughing, Rest Machining, and Finishing). The coolant used for each milling operation was Synergy 735 (Blaser Swisslube, Switzerland) (Figure 3.7A) which consists of a blend of polyglycols, mixed in a standardized ratio of approximately 1:9 (coolant to tap water ratio) with the concentration of 10%, as per the manufacturer's recommendation (Appendix B). The coolant concentration was measured by handheld refractometer (ATC, China) (Figure 3.7B).

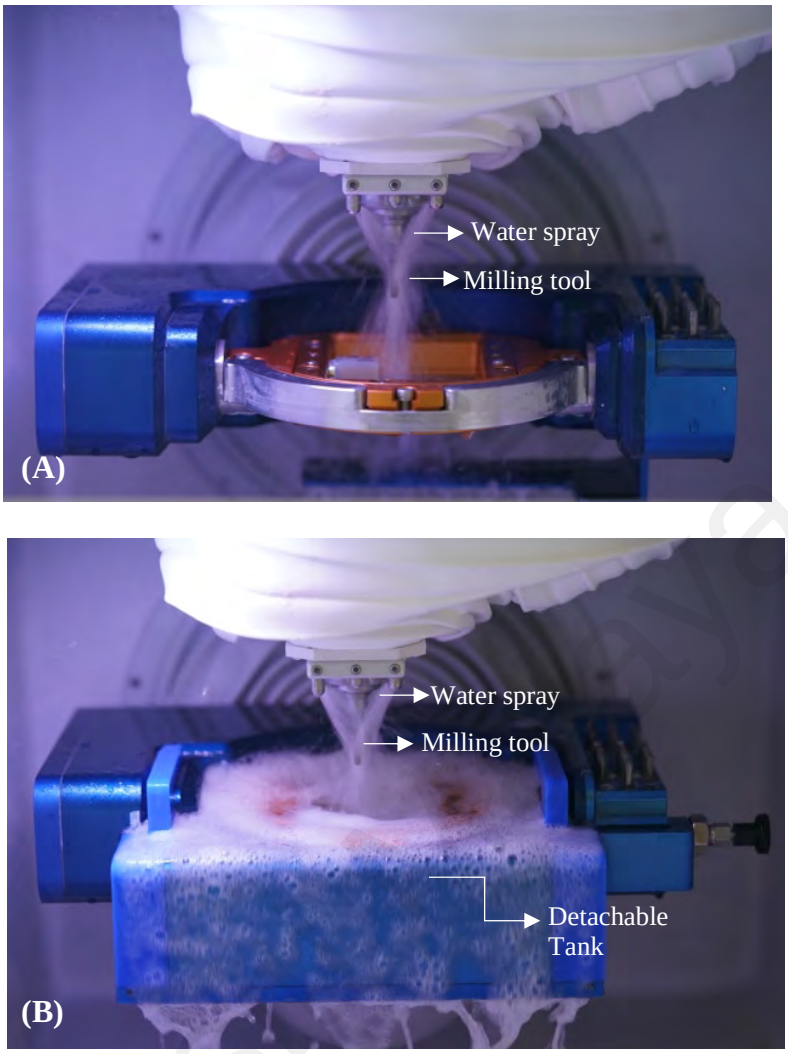

Figure 3.6: Milling techniques (A) Wet milling; (B) Submerged milling

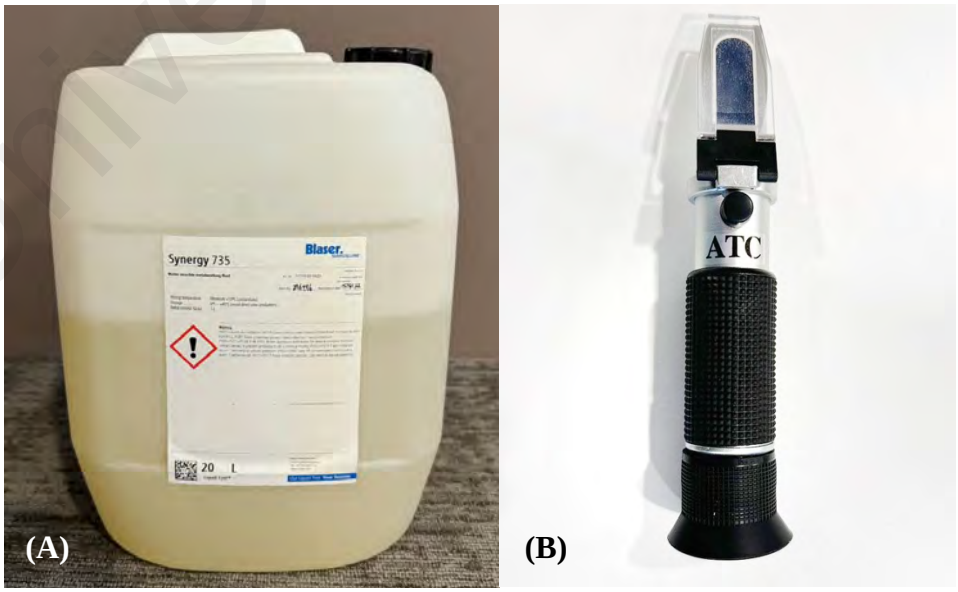

Figure 3.7: (A) Synergy 735 coolant (B) Refractometer

All samples were milled to vertical flat disc shape with a diameter of 10 mm and thickness of 2 mm with connector attached to the block (Figure 3.8). Specimens were detached from the block using a low-speed precision cutting machine Micracut 125 (Metkon Instruments Inc.) (Figure 3.9) to obtain samples measuring 10 mm diameter x 2 mm thickness (Figure 3.10). The discs were then labelled as Disc 1 to Disc 12 according to sequence of milling.

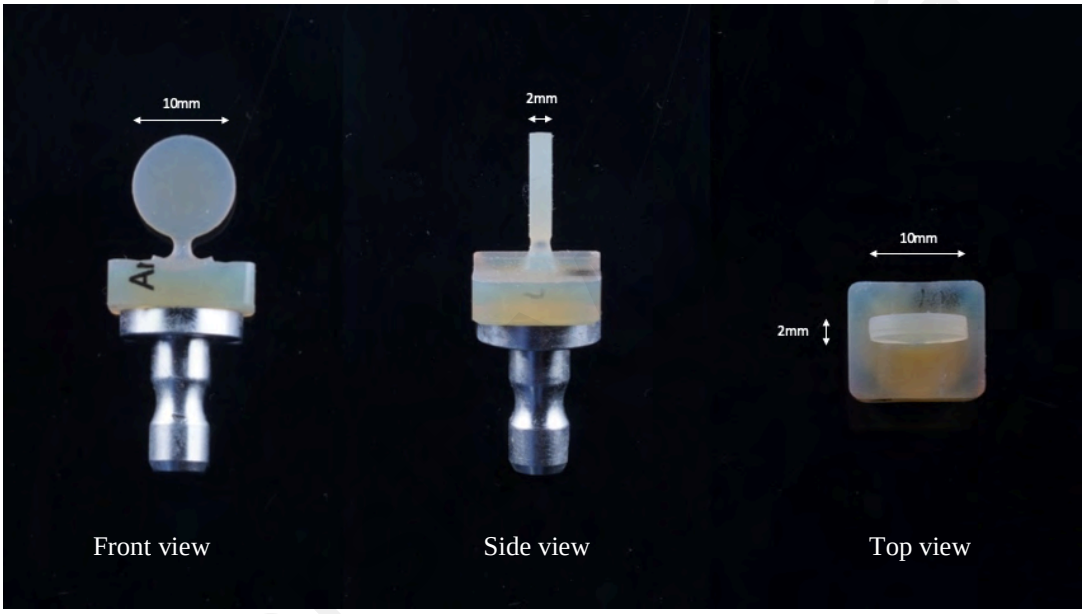

Figure 3.8: Ceramic disc dimension used in this study

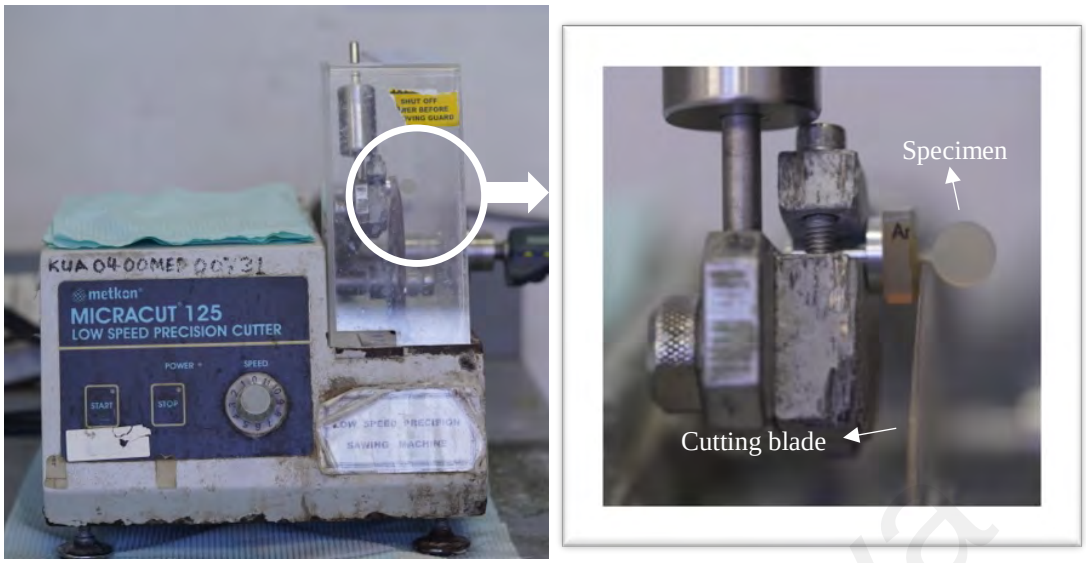

Figure 3.9: Metkon Micracut® 125 Low Speed Precision Cutter

Figure 3.10: Final lithium disilicate disc specimen

3.5 Milling tool morphology with sequential usage

New milling burs (GC 25, GC 20, and GC 10) were observed using Scanning Electron Microscope (FE-SEM SU8030, Hitachi) under low magnification of x25, x70 and x150 (only for GC 10) without gold/platinum sputtering (Figure 3.11). All milling tools were ultrasonically cleaned (distilled water; 1min) to remove debris (Figure 3.12) and dried overnight before SEM analysis. All the tools were observed again after milling Disc 1,

Disc 6, and Disc 12 for each group, which is the first, the middle, and last sample of the group. During SEM, the milling burs are set with the shank extension facing downward to standardise the area of observation (Figure 3.13A). The area that is 1 mm from the bur's tip is observed (Figure 3.13B). Based on Millbox software simulation, the first 5 mm from the tip is the most used when milling the disc shaped specimen from Amber ® Mill lithium disilicate blocks (Figure 3.14).

Figure 3.11: Field Emission Scanning Electron Microscopy (SEM) analysis (FE-SEM SU8030, Hitachi)

Figure 3.12: Whaledent Biosonic Ultrasonic Cleaner

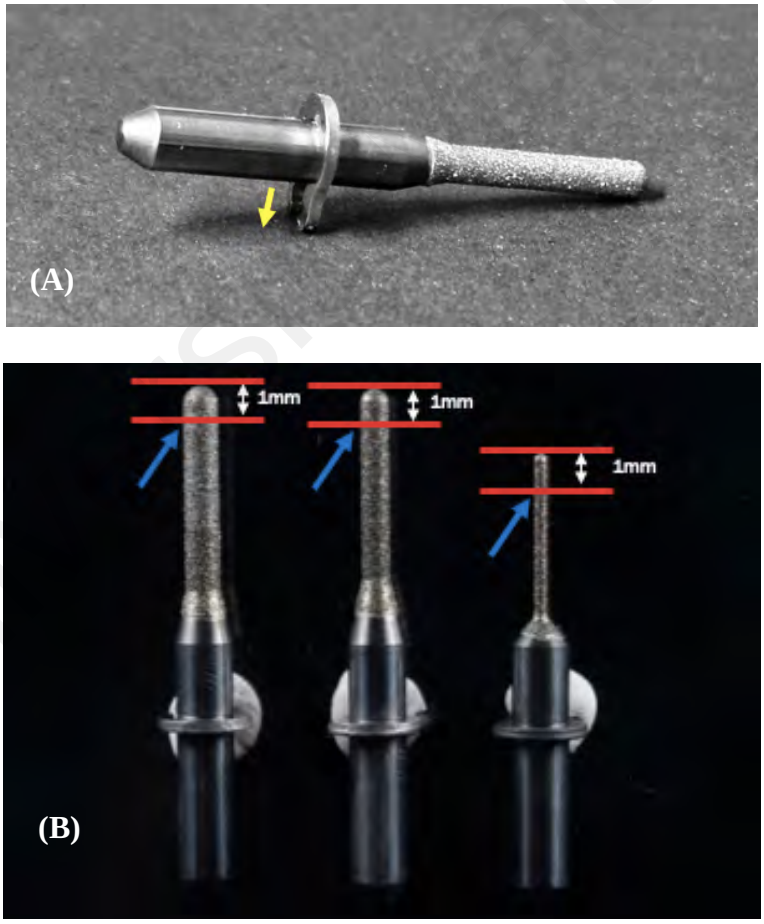

Figure 3.13: (A) Milling burs set with the shank extension facing downward to standardise the area of SEM observation; (B) 1mm of the tip of each milling bur is observed under SEM

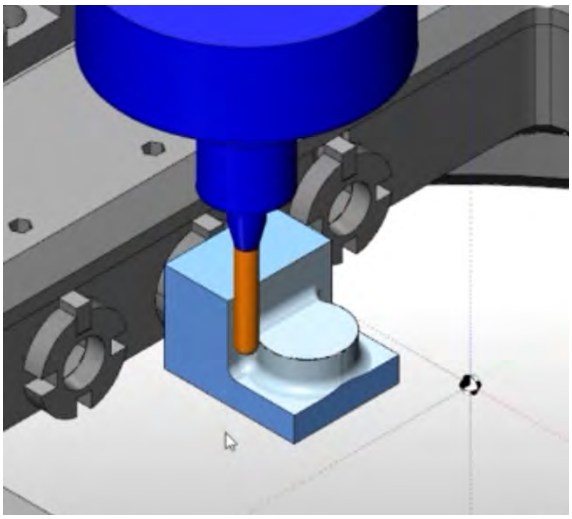

Figure 3.14: Milling simulation in Millbox software

3.6 Surface roughness of lithium disilicate

Prior to surface roughness measurements, all discs were ultrasonically cleaned (ethanol 95%; 1min) to remove debris and lubricating oil used during milling process, then dried overnight. A total of 120 measurements were performed on all 24 lithium disilicate discs. Surface roughness (Ra) data was collected using a 3D optical non-contact type surface profilometer (Alicona Infinite Focus, Olympus) under the following test conditions: magnification x20, vertical resolutions of 336 nm and lateral resolutions of 2.93 μm (Figure 3.15). Five measurements per specimen (Figure 3.16) were made (Area A, B, C, D, E) only on one side of the specimen to describe the overall roughness of the surface. The mean score of these five Ra values per specimen were calculated. The process was repeated with the same sample after the crystallization process.

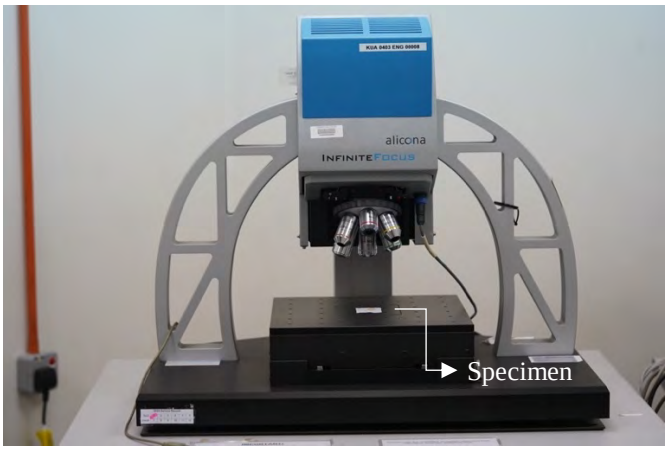

Figure 3.15: 3D optical non-contact type surface profilometer (Alicona Infinite Focus, Olympus)

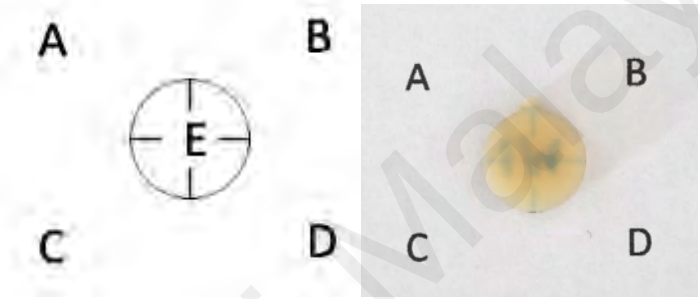

Figure 3.16: Template for surface roughness measurement area (A, B, C, D, E-middle) for each specimen

3.7 Surface morphology of lithium disilicate

For all groups, Disc 1, Disc 6, and Disc 12 were observed under SEM for the surface morphology. The discs were ultrasonically cleaned (ethanol 95%; 1min) to remove debris and lubricating oil used during milling process (Figure 3.12). They are then dried overnight for Field Emission Scanning Electron Microscopy (SEM) analysis (FE-SEM SU8030, Hitachi) under magnification of x500 without gold/platinum sputtering (Figure 3.11). The SEM images of lithium disilicate morphology was consistently taken at the center of the disc (Figure 3.17). The process was repeated with the same disc after the crystallization process. The topographic observations of the surface of milled lithium disilicate disc were compared as a complement to the quantitative results obtained with surface roughness assessment.

Figure 3.17: SEM images were taken approximately at the centre of each disc.

3.8 Crystallization of lithium disilicate

Following machining and after initial external surface roughness (Ra) measurements and Field Emission Scanning Electron Microscopy (SEM) imaging, specimens were subjected to a thermal treatment according to individual substrate manufacturer's instructions (Appendix B) using Programat EP 5000 (Ivoclar Vivadent), which is a ceramic and crystallization furnace for dentistry (Figure 3.18). Due to the correlation between crystallization temperature and the translucency of Amber Mill ® lithium disilicate blocks, all specimens were subjected to the standard crystallization parameter of HT (high translucency). With the starting temperature of 400°C for the first 3 minutes, specimens were heated up to 815°C (for HT) for 15 minutes, then cooled down slowly to room temperature in 1 hour. All specimens were marked with IPS Ivocolor Essence (Ivoclar Vivadent) E18 Black ceramic stain prior to heat treatment to allow reorientation after crystallization (Figure 3.19). Marked opacity and color changes on the discs were noted before and after crystallization (Figure 3.20).

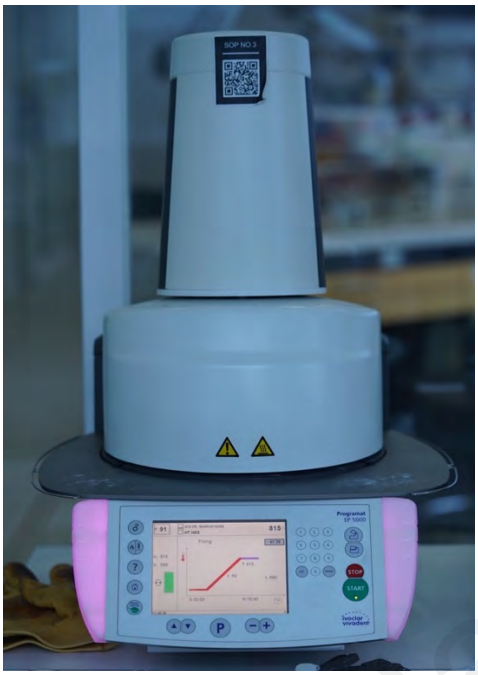

Figure 3.18: Programat EP 5000 (Ivoclar Vivadent)

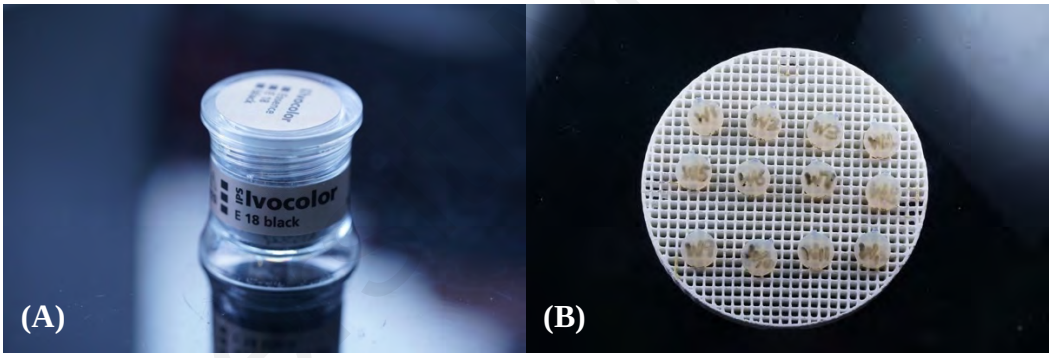

Figure 3.19: (A) IPS Ivocolor Essence (Ivoclar Vivadent) in shade E18 black; (B) Marked specimens

Figure 3.20: Lithium disilicate disc specimens. Left: Pre-crystallized; right: Post-crystallized.

3.9 Statistical Analysis

The data were analysed using Statistical Program for Social Sciences software (SPSS, Version 29 IBM, NY, USA). According to the Kolmogorov-Smirnov test, the data were normally distributed for both groups. Paired T-test was used to determine if there was a statistical difference for surface roughness (Ra) of lithium disilicate based glass ceramics milled by two different milling techniques. Meanwhile, the results for surface roughness (Ra) of glass ceramics before and after crystallization within the same milling group were analyze by Paired T-Test. One-way ANOVA was used to identify any significant difference intragroup. A *p*-value of less than 0.05 ($p < 0.05$) was considered statistically significant among group comparisons. Findings in SEM for milling burs and lithium disilicate discs are analyzed qualitatively.

CHAPTER 4: RESULTS

4.1 Surface roughness of lithium disilicate disc of wet and submerged group

This section shows the results for mean surface roughness, Ra, of lithium disilicate disc for wet milling group (before and after crystallization) and Ra for submerged group (before and after crystallization). The results were further analyzed with statistical analysis and complemented with SEM images of discs.

4.1.1 Wet Milling group (before and after crystallization)

Table 4.1: Mean Surface roughness Ra (µm) of lithium disilicate disc in wet milling group)

Disc Milling Sequence	Wet Milling (n = 12)		
	Pre-crystallization Ra mean ± SD (µm)	Post-crystallization Ra mean ± SD (µm)	Mean difference (Pre-post) (µm)
Disc 1	0.6574 ± 0.0542	0.5526 ± 0.1164	0.1048
Disc 2	0.5728 ± 0.1055	0.5896 ± 0.0926	-0.0168
Disc 3	0.6650 ± 0.1336	0.5712 ± 0.0518	0.0938
Disc 4	0.7170 ± 0.1318	0.6034 ± 0.2064	0.1136
Disc 5	0.6828 ± 0.0633	0.6630 ± 0.2046	0.0198
Disc 6	0.6700 ± 0.1335	0.6178 ± 0.1304	0.0522
Disc 7	0.7358 ± 0.0969	0.6296 ± 0.0404	0.1062
Disc 8	0.6360 ± 0.1531	0.5916 ± 0.0312	0.0444
Disc 9	0.6268 ± 0.0674	0.5276 ± 0.0876	0.0992
Disc 10	0.6670 ± 0.0639	0.5982 ± 0.0949	0.0688
Disc 11	0.7040 ± 0.1449	0.6372 ± 0.0701	0.0668
Disc 12	0.6954 ± 0.1304	0.6352 ± 0.1599	0.0602
Total Mean	0.6692	0.6014	

Table 4.2: Paired T-test for pre- and post- crystallization surface roughness (Ra)- Wet milling

Surface roughness outcome	Result
Wet Ra (pre-crystallize) x Wet Ra (post-crystallize)	$p < 0.001$, $t = 3.344$
Abbreviations: *p*, *p*-value; *t*, *t*-value	

Table 4.1 provides information about the results of the mean and standard deviation surface roughness (Ra) of the milled lithium disilicate discs in wet milling group before and after crystallization and their mean differences. The output data can be found in Appendix A. Generally, for majority of the discs in the group, Ra for pre-crystallization were higher than post-crystallization and the difference was significant ($p < 0.001$, t = 3.344) (Table 4.2), with the exception of Disc 2 in wet milling group (Ra pre-crystallization: 0.5728 ± 0.1055; Ra post-crystallization: 0.5896 ± 0.0926). However, the difference of Ra in Disc 2 was not statistically significant ($p = 0.761$).

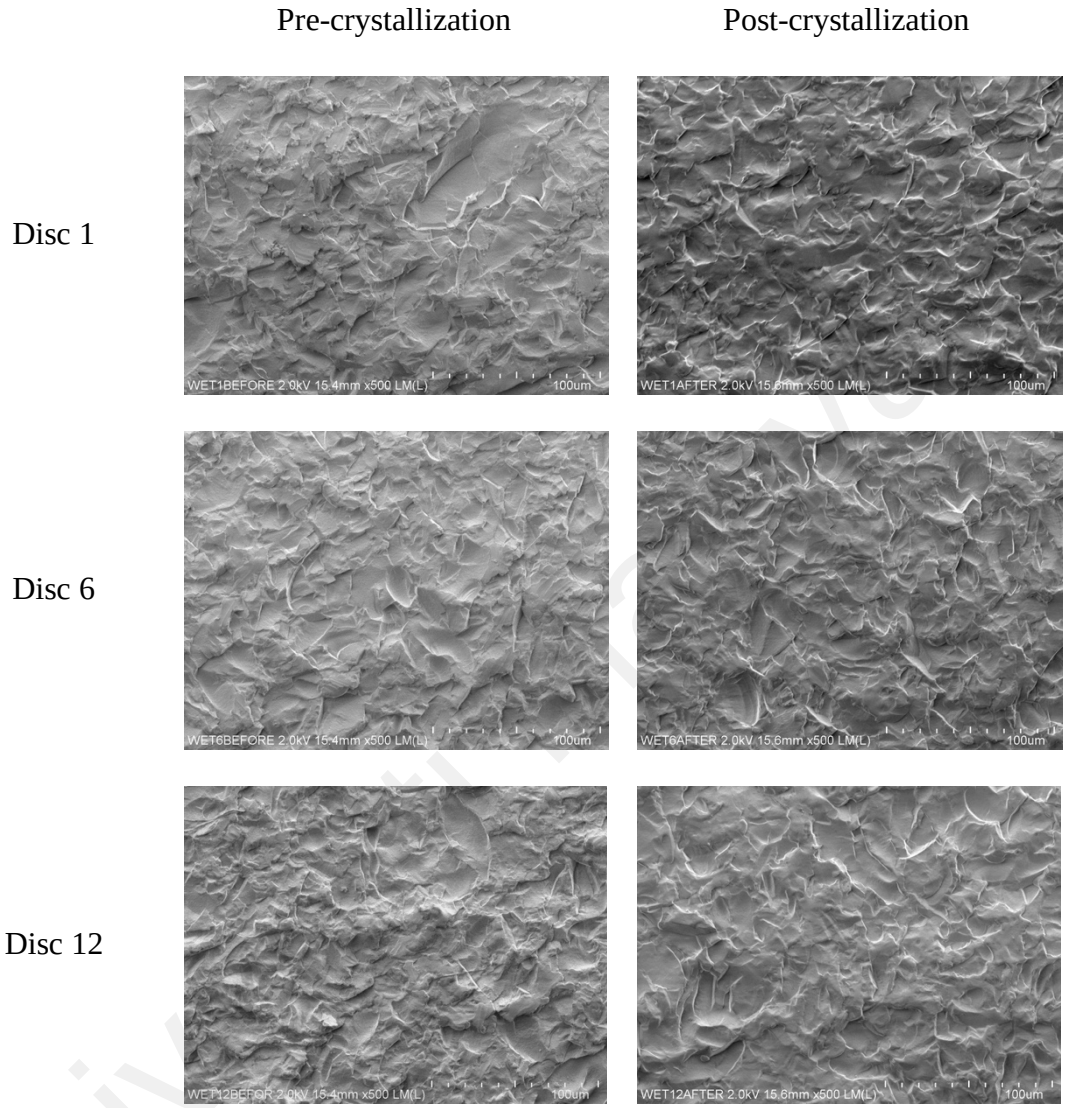

Figure 4.1: SEM images of surface morphology of lithium disilicate disc milled with wet milling under x500 magnification

Figure 4.1 shows the surface morphology of lithium disilicate disc pre- and post-crystallization, milled at 1st mill, 6th mill and 12th mill with wet milling under x500 magnification. For Disc 1, Disc 6 and Disc 12, based on the images, the changes in surface roughness pre- and post- crystallization was not apparent. However, the Ra value shown in Table 4.1 seemed to indicate a small reduction in surface roughness after crystallization.

4.1.2 Submerged Milling group (before and after crystallization)

Table 4.3 Mean Surface roughness Ra (μm) of lithium disilicate disc in submerged milling group

Disc Milling Sequence	Submerged Milling (n = 12)		
	Pre- crystallization Ra mean ± SD (μm)	Post-crystallization Ra mean ± SD (μm)	Mean difference (Pre-Post) (μm)
Disc 1	0.5606 ± 0.0905	0.5142 ± 0.0667	0.0464
Disc 2	0.5698 ± 0.0858	0.4576 ± 0.0555	0.1122
Disc 3	0.5018 ± 0.0783	0.4972 ± 0.0306	0.0046
Disc 4	0.5630 ± 0.0650	0.4872 ± 0.1136	0.0758
Disc 5	0.5974 ± 0.0463	0.5054 ± 0.0782	0.0920
Disc 6	0.5174 ± 0.0487	0.4446 ± 0.0590	0.0728
Disc 7	0.4748 ± 0.0736	0.5248 ± 0.0818	-0.0500
Disc 8	0.5596 ± 0.0600	0.5138 ± 0.1018	0.0458
Disc 9	0.5088 ± 0.0775	0.4912 ± 0.0304	0.0176
Disc 10	0.6008 ± 0.1123	0.4934 ± 0.0798	0.1074
Disc 11	0.5444 ± 0.1218	0.4614 ± 0.0758	0.0830
Disc 12	0.5710 ± 0.0665	0.4018 ± 0.0605	0.1692
Total Mean	0.5475	0.4827	

Table 4.4: Paired T-test for pre- and post- crystallization surface roughness (Ra) – Submerged milling

Surface roughness outcome	Result
Submerged Ra (pre-crystallize) x Submerged Ra (post-crystallize)	$p < 0.001$, $t = 4.683$
Abbreviations: *p*, *p*-value; *t*, *t*-value	

Table 4.3 shows information about the results of the mean and standard deviation surface roughness (Ra) of the milled lithium disilicate discs in submerged milling group before and after crystallization and their mean differences. The output data can be found in Appendix A. According to Table 4.3, Ra for pre-crystallization was overall higher than post-crystallization and the difference was significant ($p < 0.001$, $t = 4.683$) (Table 4.4), with the exception of Disc 7 in submerged milling group (Ra pre-crystallization value of 0.4748 ± 0.0736 µm; Ra post-crystallization of 0.5248 ± 0.0818 µm). The difference in Ra of Disc 7 was not statistically significant ($p = 0.324$).

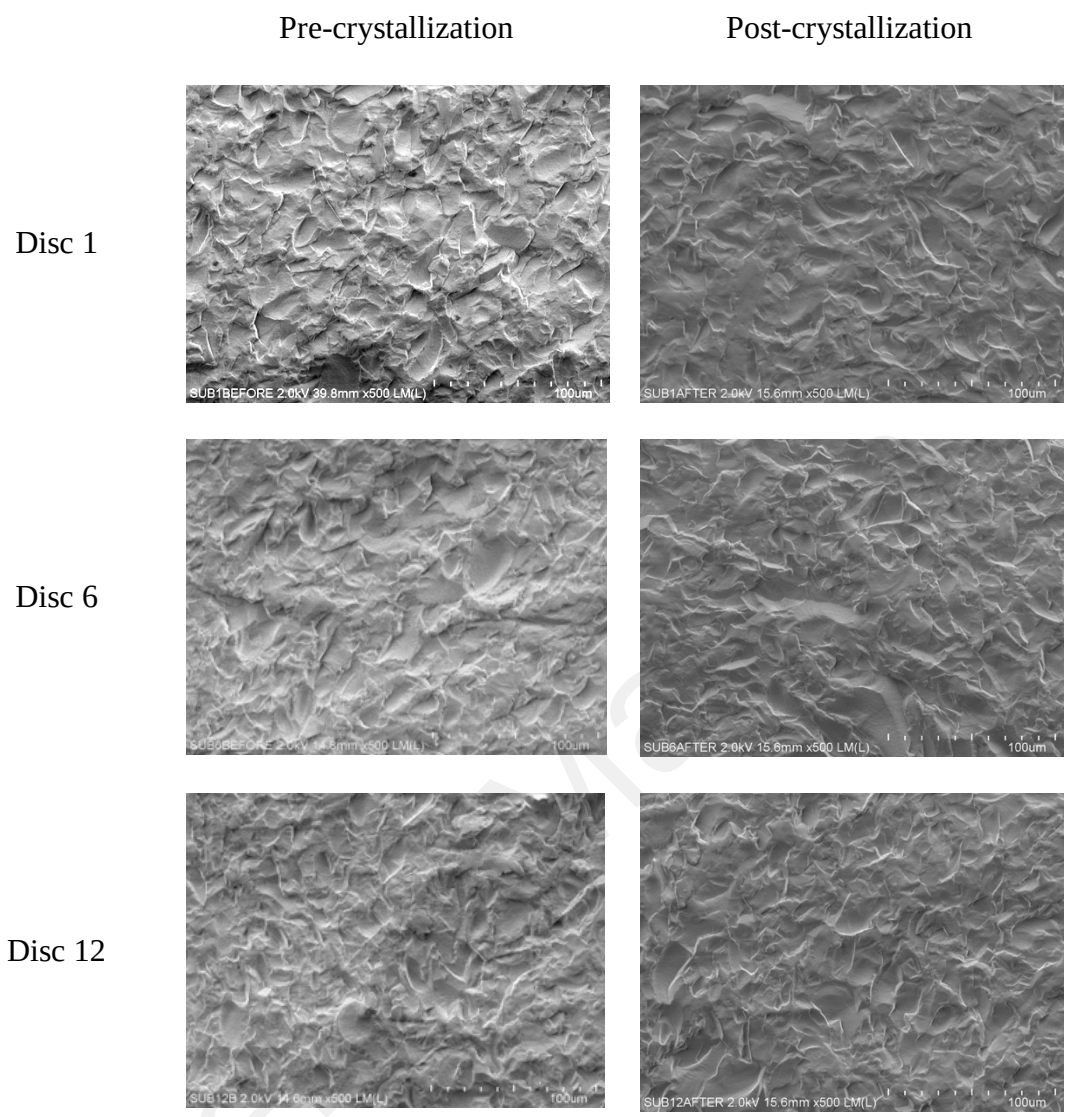

Figure 4.2: SEM images of surface morphology of lithium disilicate disc milled with submerged milling under x500 magnification

Figure 4.2 shows the surface morphology of lithium disilicate disc pre- and post-crystallization, milled at 1st mill, 6th mill and 12th mill with submerged milling under x500 magnification. For Disc 1, Disc 6 and Disc 12, based on the images, the changes in surface roughness pre- and post- crystallization was not apparent. However, the Ra value shown in Table 4.3 showed a small reduction in surface roughness after crystallization.

4.2 Surface roughness of lithium disilicate disc with sequential milling

This section shows the results for Ra with sequential milling for wet milling group and submerged milling group portrayed as line graphs and complemented with SEM images of milling burs. The results were further analyzed with statistical analysis.

4.2.1 Wet milling

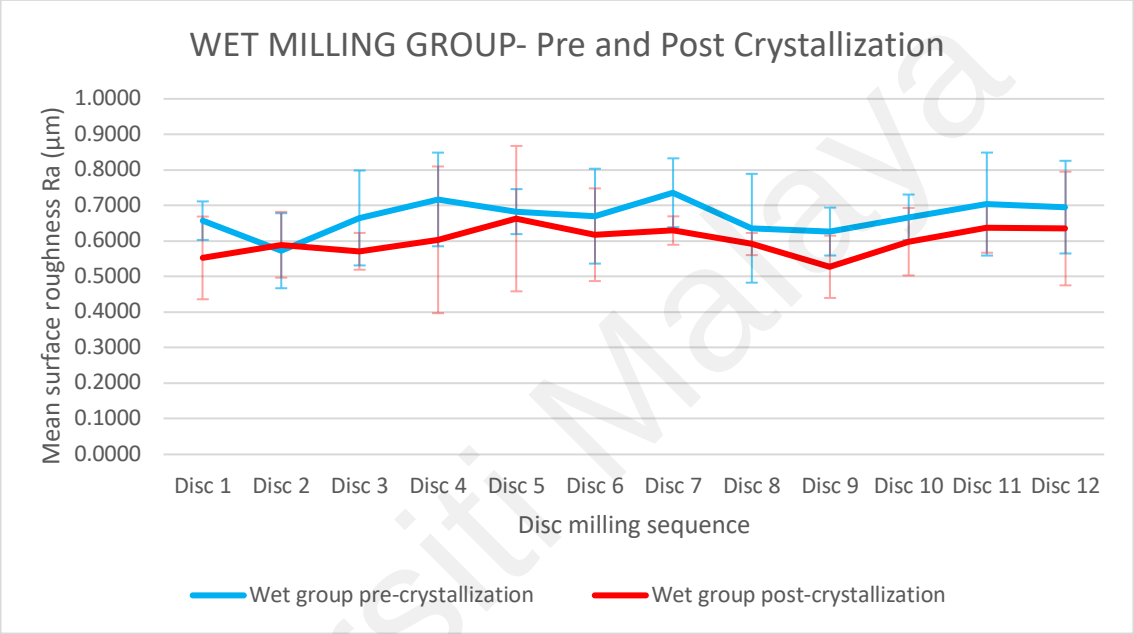

Figure 4.3: Mean surface roughness and standard error values (µm) pre- and post-crystallization in wet milling group

Table 4.5: One-way ANOVA for intragroup surface roughness (Ra) - Wet milling

Surface roughness outcome	Results
Wet Ra (pre-crystallize)	p = 0.167, F = 1.684
Wet Ra (post-crystallize)	p = 0.879, F = 0.297

Abbreviations: p, p-value; F, F-value

Figure 4.3 illustrates the surface roughness of lithium disilicate disc in wet milling group up to 12th milling. The Ra of discs showed fluctuation from 1st mill to 12th mill cycle instead of a constant upward or downward trend. Statistically, there was no significant difference between disc 1 to disc 12 in wet milling group pre-crystallized (p = 0.167, F = 1.684) and wet milling post-crystallized (p = 0.879, F = 0.297) (Table 4.5).

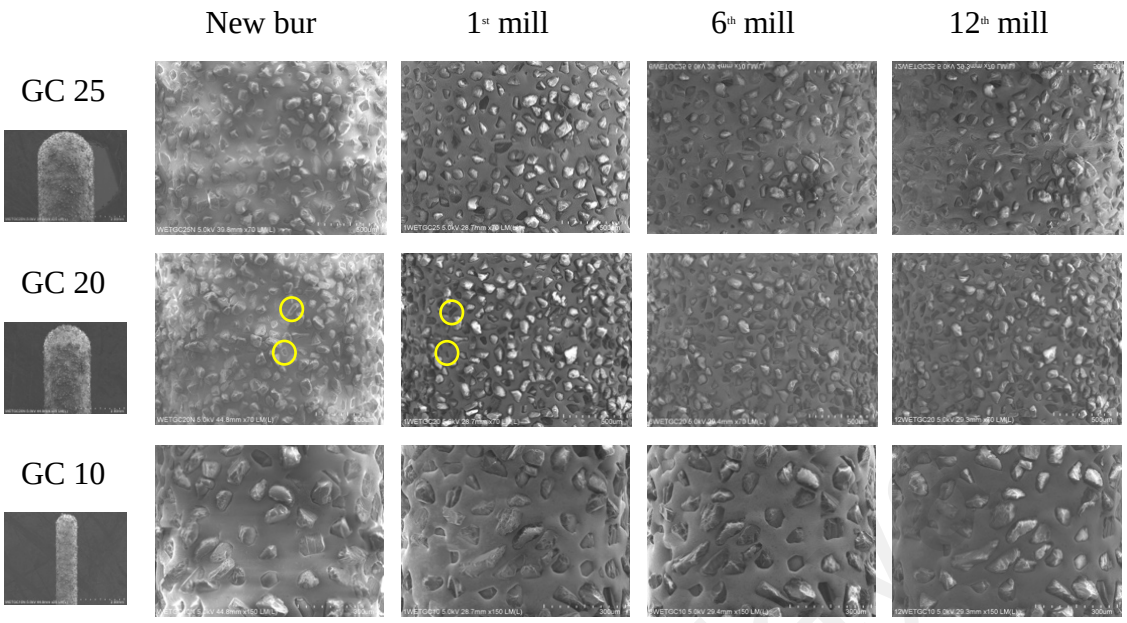

Figure 4.4: SEM images of diamond tools used in milling lithium disilicate blocks under wet milling under x70 magnification (for GC 25 and GC 20) and x150 (for GC 10). Yellow circles indicate loss of diamond abrasive particles.

Figure 4.4 illustrates SEM images of three milling tools (GC 10, GC 20, GC 25) in wet milling group at new and used state (1st, 6th and 12th mill). Loss of abrasive particles on the diamond milling tool was observed within 12 milling cycle.

4.2.2 Submerged milling

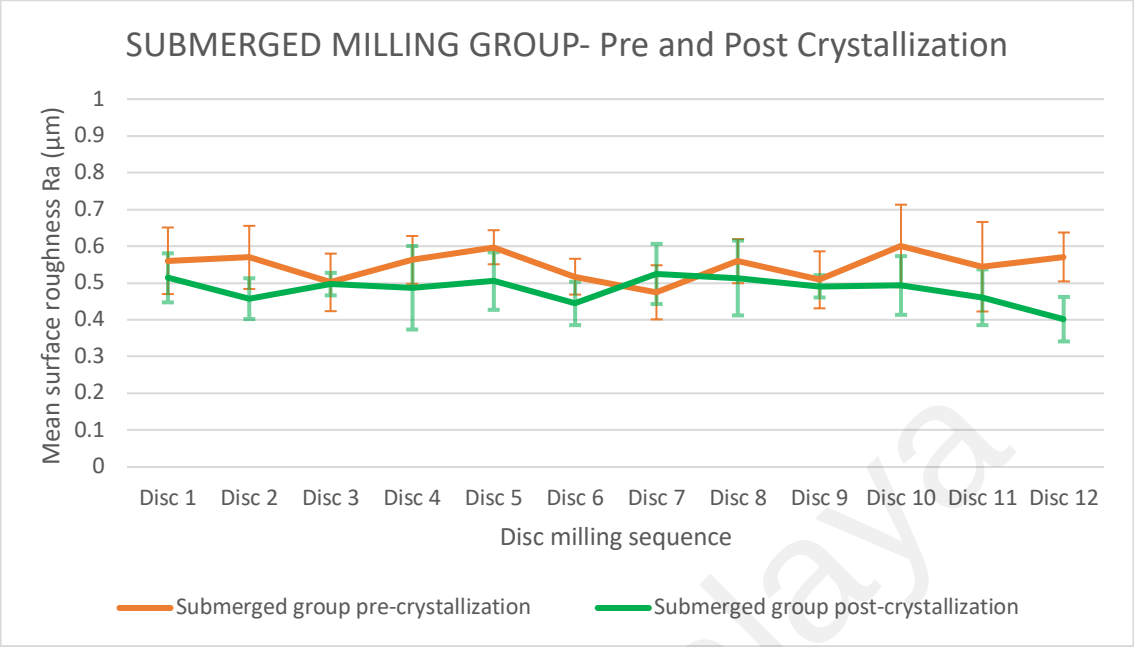

Figure 4.5: Mean surface roughness and standard error values (µm) pre- and post-crystallization in submerged milling group

Table 4.6: One-way ANOVA for intragroup surface roughness (Ra) - Submerged milling

Surface roughness outcome	Result
Submerged Ra (pre-crystallize)	p = 0.411, F = 1.009
Submerged Ra (post-crystallize)	p = 0.392, F = 1.046

Abbreviations: p, p-value; F, F-value

Figure 4.5 provides information about the surface roughness of lithium disilicate disc in submerged milling group with up to 12th milling. The Ra of discs showed no steady trend from 1st mill to 12th mill cycle. It was shown that there was no significant difference between disc 1 to disc 12 in submerged milling group pre-crystallized (p = 0.411, F = 1.009) and submerged milling group post-crystallized (p = 0.392, F = 1.046) (Table 4.6).

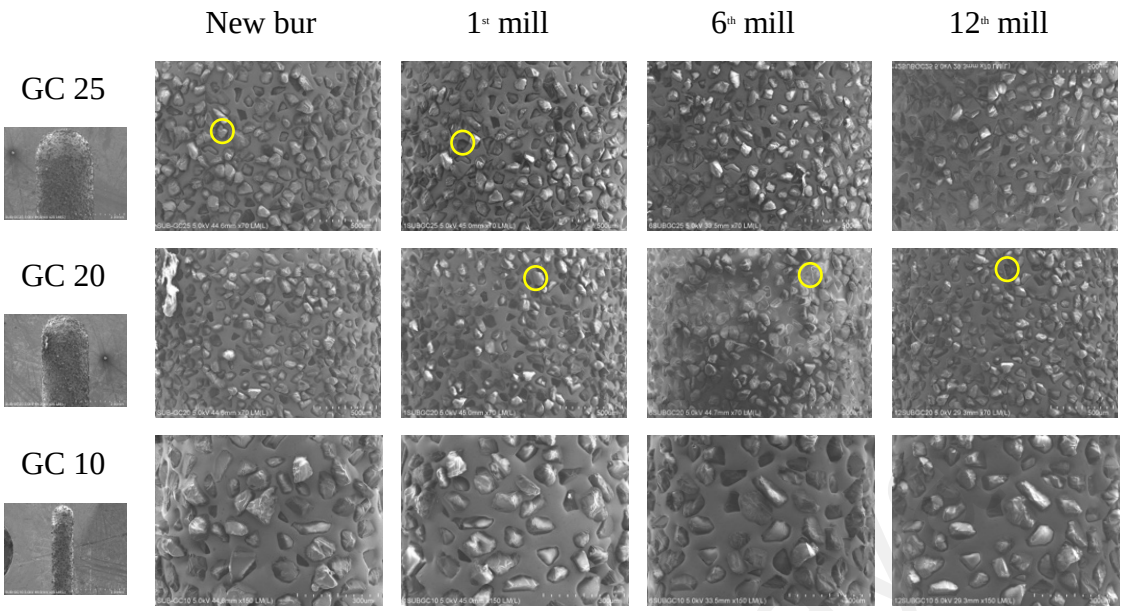

Figure 4.6: SEM images of diamond tools used in milling lithium disilicate blocks under submerged milling under x70 magnification (for GC 25 and GC 20) and x150 (for GC 10). Yellow circles indicate loss of diamond abrasive particles.

Figure 4.6 illustrates SEM images of three milling tools (GC 10, GC 20, GC 25) in submerged milling group at new and used state (1st, 6th and 12th mill). Loss of abrasive particles on the diamond milling tool was observed within 12 milling cycle.

4.3 Comparison of surface roughness of lithium disilicate milled by wet and submerged milling techniques

This section compares overall mean surface roughness Ra of lithium disilicate between the two milling groups. The result was analyzed with Paired T-test.

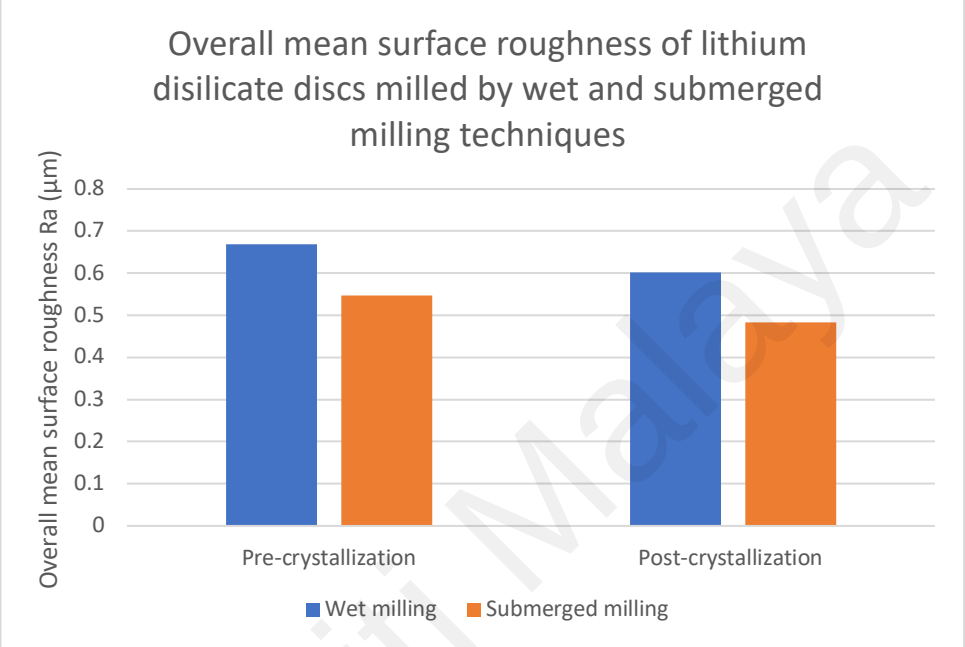

Figure 4.7: Overall mean surface roughness of lithium disilicate discs of wet and submerged milling group

Table 4.7: Paired T-test for overall mean surface roughness (Ra)

Surface roughness outcome	Results
Wet Ra (pre-crystallize) x Submerged Ra (pre-crystallize)	$p < 0.001$, t = 7.093
Wet Ra (post-crystallize) x Submerged Ra (post-crystallize)	$p < 0.001$, t = 6.020

Abbreviations: *p*, *p*-value; t, t-value

Figure 4.7 shows that overall mean surface roughness of lithium disilicate discs for wet milling group is higher than that of submerged milling group, and difference between the pre- and post-crystallization of two groups are significant (pre-crystallization $p < 0.001$, $t = 7.09$; post-crystallization $p < 0.001$, $t = 6.020$) (Table 4.7).

CHAPTER 5: DISCUSSION

5.1 Methodology

5.1.1 Surface roughness assessment

Profile parameters (indicated by the letter R followed by another character) relate to measurements of roughness along a line, calculated using a roughness profile obtained from a 2D measurement process such as stylus profilometry. One example of profile parameters is Ra (average roughness or average profile height deviations from mean line).

Areal parameters (indicated by the letter S followed by another character) relate to measurements across a surface to determine surface texture. Optical non-contact techniques can be used for areal measurements. One example of areal parameters is Sa (arithmetic mean height of the surface). Sa is the average height of all measured points in the areal (3D) measurement, calculated across the entire area of dataset.

We decided to utilize Ra for this study since the majority of previous research on the surface roughness of glass ceramics utilized Ra as the parameter for measuring surface roughness (Owen Addison et al., 2012; Alves et al., 2022; Brodine et al., 2021; Corazza et al., 2015; Fraga et al., 2017; Madruga et al., 2019; Payaminia et al., 2021b).

5.2 Results

5.2.1 Effect of milling technique on surface roughness of lithium disilicate

Based on Figure 4.7, mean Ra of discs in the submerged milling group (both pre- and post- crystallization) is significantly lower than that of the wet milling group. The results indicate that the null hypothesis, which states that there will be no significant difference

in the surface roughness of milled lithium disilicate between wet milling and submerged milling techniques, is rejected.

Milling lithium disilicate glass ceramic with submerged milling is beneficial to reduce surface roughness of the milled product. This could be attributed to the immersion of material and the milling burs in the lubricating liquid during the milling process, which may reduce friction and increase effectiveness of debris removal from milling site. According to Naik et al. (2015), the submerged milling technique produces better surface finish because the lubricating liquid is constantly present at the interface between the milling tool and the work piece (Naik et al., 2015).

5.2.2 Effect of crystallization on surface roughness of lithium disilicate

Based on the data shown in Table 4.1 and 4.3, it is clear that the Ra values before crystallization are significantly higher than Ra values after crystallization for both wet and milling groups. Although reduction of surface roughness is not evident from SEM (Figure 4.1 and Figure 4.2), it can be concluded from Ra value that surface roughness reduced following crystallization. Hence, we reject the null hypotheses that crystallization will not have a significant effect on the surface roughness in milled lithium disilicate.

According to a previous study by Alves et al. (2022), Ra parameter undergo reduction (1.2-1.25 μm) due to the softening and smoothing of the amorphous phase present in the glass ceramic following heat treatment (Alves et al., 2022). The majority of disc specimens in this study demonstrate a reduction in surface roughness after crystallisation. While the Ra disc for pre-crystallization is typically higher than post-crystallization, there were two exceptions. In the wet milling group, Disc 2 had a Ra pre-crystallization value

of 0.5728 ± 0.1055 μm and a Ra post-crystallization value of 0.5896 ± 0.0926 μm. In the submerged milling, Disc 7 had a Ra pre-crystallization value of 0.4748 ± 0.0736 μm and a Ra post-crystallization of 0.5248 ± 0.0818 μm. For these two discs, the average Ra after crystallization is greater than before crystallization but the difference is not statistically significant.

5.2.3 Sequential milling and surface roughness of lithium disilicate

Based on the data presented in Figure 4.3 and 4.5, the average surface roughness between Disc 1 to Disc 12 within each group shows no significant difference with the milling sequence. One Way ANOVA test for intragroup comparison showed no significant difference between disc 1 to disc 12 in all the groups ($p > 0.05$). It is evident that the mean surface roughness of lithium disilicate disc does not exhibit consistent changes with the milling sequence. The mean surface roughness shows fluctuation from disc 1 to disc 12 for both groups, both before and after crystallization, without any obvious trend. It is apparent that there is no correlation between sequence of milling and the surface roughness of the milled disc up to 12th milling in our investigation. Therefore, the null hypotheses of sequential milling tool usage using wet and submerged milling techniques has no impact on surface roughness of lithium disilicate is accepted.

This finding is in accordance to a study conducted by Madruga et al. (2019) which showed that deterioration of bur due to sequential bur usage have no impact on roughness and topography of lithium disilicate ceramic surface (Madruga et al., 2019). Their finding was consistent across different milling stages, as the study measured and compared surface roughness after the 6th, 12th and 18th use the burs. Addison et al. (2012) reported that surface roughness seemed to be probabilistic. This means that the introduction of a significant

strength limiting flaw depends on a random selection of a bur and a random milling sequence (Owen Addison et al., 2012).

The milling tools used in this study were deemed to have the same composition and geometry, as they were manufactured by the same company. Nevertheless, variations in the distribution and orientation of the diamond particle-impregnated surface were observed in Figure 4.4 and 4.6. Earlier in vitro studies have demonstrated that the shape, number and size of diamond grains present in the milling burs have an impact on the mechanical properties of the machined material. Additionally, it has been observed that the diamond grains are worn or loss with the use of the bur (Owen Addison et al., 2012; Sakoda et al., 2018; Tomita et al., 2005). Madruga et al. (2019) showed clear differences in both quantity and shape of the diamonds grains when comparing them from the start and end of each milling process (Madruga et al., 2019). On the other hand, Tomita et al. (2005) observed that the diamond bur showed a rise in the loss of abrasive particles throughout the 11^{th} to 21^{st} machining processes (Tomita et al., 2005). In the current study, loss of abrasive particles on milling bur was observed on SEM in both groups. However, only a small area of each milling burs was observed and milling is only limited up to 12 cycles in this study.

5.3 Limitations of study

Main limitation of the study was the limited number of repeated use (12 cycles) of milling burs and production of specimens for each group. This may not be sufficient to observe significant changes in the surface roughness of the specimens within the same group and abrasive particles loss on milling burs with sequential milling. In addition, only one kind of material was investigated in this study. Surface roughness can vary amongst CAD/CAM materials manufactured by different companies due to the differences in their microstructure. Another constraint of this study was that it only examined round flat disc-shaped specimen. Other types of restoration shapes, such as veneers and onlays, may have different machined surface area, which may result in variation in surface roughness. Furthermore, the SEM examination of a small area of the milling burs may not have been adequate to observe the overall loss of abrasive particles on the milling burs.

CHAPTER 6: CONCLUSIONS

6.1 Conclusion

Within the limitations of this study, based on the findings, the following conclusion can be drawn:

1. Submerged milling technique can significantly reduce the surface roughness of lithium disilicate compared to wet milling technique.
2. Crystallization significantly reduced the surface roughness of machinable lithium disilicate glass ceramic in both wet and submerged milling groups.
3. Sequential tool usage up to 12^{th} mill had no impact on surface roughness of lithium disilicate in both wet and submerged milling groups.

6.2 Recommendations for future studies

For further researches,

1. To increase number of milling cycles.
2. To include CAD/CAM materials with varying compositions from different manufacturers.
3. To mill various forms of restorations, such as onlay or veneer specimens.
4. To observe larger surface area of milling burs for better examination of abrasive particles.

REFERENCES

Addison, O., Cao, X., Sunnar, P., & Fleming, G. J. P. (2012). Machining variability impacts on the strength of a 'chair-side' CAD–CAM ceramic. *Dental Materials, 28*(8), 880-887.

Ahlers, M. O., Mörig, G., Blunck, U., Hajtó, J., Pröbster, L., & Frankenberger, R. (2009). Guidelines for the preparation of CAD/CAM ceramic inlays and partial crowns. *International journal of computerized dentistry, 12*(4), 309-325.

Al-Marzok, M. I., & Al-Azzawi, H. J. (2009). The effect of the surface roughness of porcelain on the adhesion of oral Streptococcus mutans. *The Journal of Contemporary Dental Practice, 10*(6), E017-024.

Alao, A.-R., Stoll, R., Song, X.-F., Abbott, J. R., Zhang, Y., Abduo, J., & Yin, L. (2017). Fracture, roughness and phase transformation in CAD/CAM milling and subsequent surface treatments of lithium metasilicate/disilicate glass-ceramics. *Journal of the Mechanical Behavior of Biomedical Materials, 74*, 251-260.

Alves, M. F., Simba, B., Campos, L., Ferreira, I., & Santos, C. (2019). Influence of heat-treatment protocols on mechanical behavior of lithium silicate dental ceramics. *International Journal of Applied Ceramic Technology, 16*.

Alves, M. F., Simba, B. G., Fernandes, M. H. V., Elias, C., Amarante, J. E., & Santos, C. (2022). Effect of Roughness on Flexural Strength of Dental Lithium-Disilicate. *Dental Materials, 38*, e3.

Belli, R., Lohbauer, U., Goetz-Neunhoeffer, F., & Hurle, K. (2019). Crack-healing during two-stage crystallization of biomedical lithium (di)silicate glass-ceramics. *Dental Materials, 35*(8), 1130-1145.

Bollen, C. M. L., Papaioanno, W., Van Eldere, J., Schepers, E., Quirynen, M., & Van Steenberghe, D. (1996). The influence of abutment surface roughness on plaque accumulation and peri-implant mucositis. *Clinical oral implants research, 7*(3), 201-211.

Brodine, B. A., Korioth, T. V., Morrow, B., Shafter, M. A., Hollis, W. C., & Cagna, D. R. (2021). Surface Roughness of Milled Lithium Disilicate With and Without Reinforcement After Finishing and Polishing: An In Vitro Study. *Journal of Prosthodontics, 30*(3), 245-251.

CAD-Ray. (2023). *DOF Craft5X Submerged Water Bath for x-tra Fast Glass milling*. https://www.cad-ray.com/product/dof-craft5x-submerged-water-bath-for-x-tra-fast-glass-milling/

Corazza, P., Castro, H., Feitosa, S., Kimpara, E., & Della Bona, A. (2015). Influence of CAD-CAM diamond bur deterioration on surface roughness and maximum failure load of Y-TZP-based restorations. *American journal of dentistry, 28*, 95-99.

Denry, I., & Holloway, J. A. (2010). Ceramics for dental applications: a review. *Materials, 3*(1), 351-368.

Dhar, N. (2005). *Cutting Temperature, Tool Wear, Surface Roughness and Dimensional Deviation in Cryogenic Machining*.

Dhar, N., Ahmed, M., & Islam, S. (2007). An experimental investigation on effect of minimum quantity lubrication in machining AISI 1040 steel. *International Journal of Machine Tools & Manufacture.*

Duarte Jr, S., Phark, J.-H., Blatz, M., & Sadan, A. (2010). Ceramic Systems: An Ultrastructural Study. *Quintessence of Dental Technology (QDT), 33*.

Duret, F., Blouin, J. L., & Duret, B. (1988). CAD-CAM in dentistry. *The Journal of the American Dental Association*, *117*(6), 715-720.

Fabian Fonzar, R., Carrabba, M., Sedda, M., Ferrari, M., Goracci, C., & Vichi, A. (2017). Flexural resistance of heat-pressed and CAD-CAM lithium disilicate with different translucencies. *Dental Materials*, *33*(1), 63-70.

Ferro, K. J., Morgano, S. M., Driscoll, C. F., Freilich, M. A., Guckes, A. D., Knoernschild, K. L., McGarry, T. J., Photography, N. A., & Twain, M. (2017). The glossary of prosthodontic terms.

Fraga, S., Amaral, M., Bottino, M. A., Valandro, L. F., Kleverlaan, C. J., & May, L. G. (2017). Impact of machining on the flexural fatigue strength of glass and polycrystalline CAD/CAM ceramics. *Dental Material*, *33*(11), 1286-1297.

Fu, Q., Beall, G. H., Smith, C. M., Kohli, J. T., Youngman, R. E., Wheaton, B. R., Credle, A. J., & Gulbiten, O. (2016). Strong, Tough Glass-Ceramics for Emerging Markets. *International Journal of Applied Glass Science*, *7*(4), 486-491.

Fuzzi, M., & Rappelli, G. (1998). Survival rate of ceramic inlays. *Journal of Dentistry*, *26*(7), 623-626.

Gracis, S., Thompson, V. P., Ferencz, J. L., Silva, N. R., & Bonfante, E. A. (2015). A new classification system for all-ceramic and ceramic-like restorative materials. *International Journal of Prosthodontics*, *28*(3), 227-235.

Guazzato, M., Albakry, M., Ringer, S. P., & Swain, M. V. (2004). Strength, fracture toughness and microstructure of a selection of all-ceramic materials. Part I. Pressable and alumina glass-infiltrated ceramics. *Dental Material*, *20*(5), 441-448.

Hallmann, L., Ulmer, P., Gerngross, M. D., Jetter, J., Mintrone, M., Lehmann, F., & Kern, M. (2019). Properties of hot-pressed lithium silicate glass-ceramics. *Dental Material*, *35*(5), 713-729.

Höland, W., Schweiger, M., Frank, M., & Rheinberger, V. (2000). A comparison of the microstructure and properties of the IPS Empress 2 and the IPS Empress glass-ceramics. *Journal of Biomedical Materials*, *53*(4), 297-303.

Hung, C. Y., Lai, Y. L., Hsieh, Y. L., Chi, L. Y., & Lee, S. Y. (2008). Effects of simulated clinical grinding and subsequent heat treatment on microcrack healing of a lithium disilicate ceramic. *The International Journal of Prosthodontics*, *21*(6), 496-498.

James, P. F. (1995). Glass ceramics: new compositions and uses. *Journal of Non-Crystalline Solids*, *181*(1), 1-15.

Kelly, J., & Benetti, P. (2011). Ceramic materials in dentistry: historical evolution and current practice. *Australian Dental Journal*, *56*(s1), 84-96.

Lien, W., Roberts, H. W., Platt, J. A., Vandewalle, K. S., Hill, T. J., & Chu, T. M. (2015). Microstructural evolution and physical behavior of a lithium disilicate glass-ceramic. *Dental Material*, *31*(8), 928-940.

Lindner, S., Frasheri, I., Hickel, R., Crispin, A., & Kessler, A. (2023). Retrospective clinical study on the performance and aesthetic outcome of pressed lithium disilicate restorations in posterior teeth up to 8.3 years. *Clinical Oral Investigations*, *27*.

Madruga, C. F. L., Bueno, M. G., Dal Piva, A. M. d. O., Prochnow, C., Pereira, G. K. R., Bottino, M. A., Valandro, L. F., & de Melo, R. M. (2019). Sequential usage of diamond bur for CAD/CAM milling: Effect on the roughness, topography and fatigue strength of lithium disilicate glass ceramic. *Journal of the Mechanical Behavior of Biomedical Materials*, *91*, 326-334.

Miranda, J. S., Barcellos, A. S. P., Campos, T. M. B., Cesar, P. F., Amaral, M., & Kimpara, E. T. (2020). Effect of repeated firings and staining on the mechanical behavior and composition of lithium disilicate. *Dental Material*, *36*(5), e149-e157.

Miyazaki, T., Hotta, Y., Kunii, J., Kuriyama, S., & Tamaki, Y. (2009). A review of dental CAD/CAM: current status and future perspectives from 20 years of experience. *Dental Materials Journal*, *28*(1), 44-56.

Mörmann, W. H. (2006). The evolution of the CEREC system. The *Journal of the American Dental Association*, *137 Supplement*, 7s-13s.

Mörmann, W. H., & Brandestini, M. (1987). [Cerec-System: computerized inlays, onlays and shell veneers]. *Zahnarztl Mitt*, *77*(21), 2400-2405. (Cerec-System: Computer-Inlays, -Onlays und -Schalenverblendungen.)

Naik, R. R., Gaekwad, S., & Naik, R. (2015). Design of a submerged cooling system for a vertical axis CNC milling machine. *International Journal of Engineering and Innovative Technology (IJEIT)*, *5*, 53-56.

Nawafleh, N. A., Hatamleh, M. M., Öchsner, A., & Mack, F. (2017). Fracture load and survival of anatomically representative monolithic lithium disilicate crowns with reduced tooth preparation and ceramic thickness. *Journal of Advanced Prosthodontics*, *9*(6), 416-422.

Ortiz, A. L., Borrero-López, O., Guiberteau, F., & Zhang, Y. (2019). Microstructural development during heat treatment of a commercially available dental-grade lithium disilicate glass-ceramic. *Dental Materials*, *35*(5), 697-708.

Pacha-Olivenza, M. Á., Tejero, R., Fernández-Calderón, M. C., Anitua, E., Troya, M., & González-Martín, M. L. (2019). Relevance of Topographic Parameters on the Adhesion and Proliferation of Human Gingival Fibroblasts and Oral Bacterial Strains. *BioMed Research International*, *2019*, 8456342.

Payaminia, L., Moslemian, N., Younespour, S., Koulivand, S., & Alikhasi, M. (2021a). Evaluating the effect of repeated use of milling burs on surface roughness and adaptation of digitally fabricated ceramic veneers. *Heliyon*, *7*(4), e06896.

Pereira, G. K. R., Silvestri, T., Amaral, M., Rippe, M. P., Kleverlaan, C. J., & Valandro, L. F. (2016). Fatigue limit of polycrystalline zirconium oxide ceramics: Effect of grinding and low-temperature aging. *Journal of the Mechanical Behaviour Biomedical Materials*, *61*, 45-54.

Phark, J. H., & Duarte, S., Jr. (2022). Microstructural considerations for novel lithium disilicate glass ceramics: A review. *Journal of Esthetic and Restorative Dentistry*, *34*(1), 92-103.

Pilecco, R. O., Dalla-Nora, F., Guilardi, L. F., Pereira, G. K. R., de Andrade, G. S., de Melo, R. M., Valandro, L. F., & Rippe, M. P. (2021). In-lab simulation of CAD/CAM milling of lithium disilicate glass-ceramic specimens: Effect on the fatigue behavior of the bonded ceramic. *Journal of the Mechanical Behavior of Biomedical Materials*, *121*, 104604.

Quinn, G., Ives, L., & Jahanmir, S. (2005). On the nature of machining cracks in ground ceramics: Part I: SRBSN strengths and fractographic analysis. *Machining Science and Technology*, *9*, 169-210.

Riquieri, H., Monteiro, J. B., Viegas, D. C., Campos, T. M. B., de Melo, R. M., & de Siqueira Ferreira Anzaloni Saavedra, G. (2018). Impact of crystallization firing process on the microstructure and flexural strength of zirconia-reinforced lithium silicate glass-ceramics. *Dental Material*, *34*(10), 1483-1491.

Sailer, I., Makarov, N. A., Thoma, D. S., Zwahlen, M., & Pjetursson, B. E. (2015). All-ceramic or metal-ceramic tooth-supported fixed dental prostheses (FDPs)? A systematic review of the survival and complication rates. Part I: Single crowns (SCs). *Dental Material*, *31*(6), 603-623.

Sakoda, S., Nakao, N., & Watanabe, I. (2018). The effect of abrading and cutting instruments on machinability of dental ceramics. *Journal of Materials Science: Materials in Medicine*, *29*(3), 34.

Sasse, M., Krummel, A., Klosa, K., & Kern, M. (2015). Influence of restoration thickness and dental bonding surface on the fracture resistance of full-coverage occlusal veneers made from lithium disilicate ceramic. *Dental Material*, *31*(8), 907-915.

Seydler, B., Rues, S., Müller, D., & Schmitter, M. (2014). In vitro fracture load of monolithic lithium disilicate ceramic molar crowns with different wall thicknesses. *Clinical Oral Investigations*, *18*(4), 1165-1171.

Simba, B., Alves, M. F., Villela, T., Ribeiro, M., Strecker, K., & Santos, C. (2022). Impact of diamond tool wear on the surface finish of lithium silicate glass ceramics machined with the assistance of CAD/CAM systems. *Journal of the Brazilian Society of Mechanical Sciences and Engineering*, *45*.

Thompson, V. P., & Rekow, D. E. (2004). Dental ceramics and the molar crown testing ground. *Journal of Applied Oral Science*, *12*, 26-36.

Tomita, S., Shin-Ya, A., Gomi, H., Matsuda, T., Katagiri, S., Shin-Ya, A., Suzuki, H., Yara, A., Ogura, H., Hotta, Y., Miyazaki, T., & Sakamoto, Y. (2005). Machining accuracy of CAD/CAM ceramic crowns fabricated with repeated machining using the same diamond bur. *Dental Material Journal*, *24*(1), 123-133.

Turon-Vinas, M., & Anglada, M. (2018). Strength and fracture toughness of zirconia dental ceramics. *Dental Material*, *34*(3), 365-375.

Yap, A. U., Lye, K. W., & Sau, C. W. (1997). Surface characteristics of tooth-colored restoratives polished utilizing different polishing systems. *Operative Dentistry*, *22*(6), 260-265.

Yara, A., Ogura, H., Shinya, A., Tomita, S., Miyazaki, T., Sugai, Y., & Sakamoto, Y. (2005). Durability of diamond burs for the fabrication of ceramic crowns using dental CAD/CAM. *Dental Material Journal*, *24*(1), 134-139.

Zanotto, E. D. (2010). Bright future for glass-ceramics. *American Ceramics Society Bulletin*, *89*(8), 19-27.

Zarone, F., Ferrari, M., Mangano, F. G., Leone, R., & Sorrentino, R. (2016). "Digitally Oriented Materials": Focus on Lithium Disilicate Ceramics. *International Journal of Dentistry, 2016*, 9840594.

Zheng Yang, K., Pramanik, A., Basak, A. K., Dong, Y., Prakash, C., Shankar, S., Dixit, S., Kumar, K., & Ivanovich Vatin, N. (2023). Application of coolants during tool-based machining – A review. *Ain Shams Engineering Journal*, *14*(1), 101830.